Georg-August-Universität Göttingen

A Functional Characterization of *Drosophila* Chordotonal Organs

Dissertation

for the award of the degree

"Doctor rerum naturalium"
of the Georg-August-Universität Göttingen

within the GGNB doctoral program
"Sensory and Motor Neuroscience"

of the Georg-August University School of Science (GAUSS)

submitted by
Robert Jago Wiek

From Münster, Germany
Göttingen 2013

Members of Thesis Committee
& Oral Examination

Prof. Dr. Martin Göpfert (Supervisor/Reviewer)
Georg-August-University of Göttingen, Cellular Neurobiology

Prof. Dr. André Fiala (Reviewer)
Georg-August-University of Göttingen, Molecular Neurobiology of Behaviour

Prof. Dr. Ansgar Büschges
University of Cologne, Neurobiology / Animal Physiology

Members Oral Examination

Prof. Dr. Andreas Stumpner
Georg-August-University of Göttingen, Neuroethology

Prof. Dr. Ralf Heinrich
Georg-August-University of Göttingen, Cellular Neurobiology

Research Group Leader Dr. Halyna Shcherbata
Max Planck Institute for Biophysical Chemistry, Gene Expression and Signaling

Oral examination: June 21.06.2013

Promovierenden-Erklärung
der Georg-August-Universität Göttingen

Name: Wiek, Robert

Anschrift: Kiefernweg 5, 37085, Göttingen

Ich beabsichtige, eine Dissertation zum Thema

"A Functional Characterization of *Drosophila* Chordotonal Organs"
an der Georg-August-Universität Göttingen anzufertigen.

Dabei werde ich von Frau/Herrn
Prof.Dr. Martin Göpfert betreut.

Ich gebe folgende Erklärung ab:

1. Die Gelegenheit zum vorliegenden Promotionsvorhaben ist mir nicht kommerziell vermittelt worden. Insbesondere habe ich keine Organisation eingeschaltet, die gegen Entgelt Betreuerinnen und Betreuer für die Anfertigung von Dissertationen sucht oder die mir obliegenden Pflichten hinsichtlich der Prüfungsleistungen für mich ganz oder teilweise erledigt.
2. Hilfe Dritter wurde bis jetzt und wird auch künftig nur in wissenschaftlich vertretbarem und prüfungsrechtlich zulässigem Ausmaß in Anspruch genommen. Insbesondere werden alle Teile der Dissertation selbst angefertigt; unzulässige fremde Hilfe habe ich dazu weder unentgeltlich noch entgeltlich entgegengenommen und werde dies auch zukünftig so halten.
3. Die Richtlinien zur Sicherung der guten wissenschaftlichen Praxis an der Universität Göttingen werden von mir beachtet.
4. Eine entsprechende Promotion wurde an keiner anderen Hochschule im In- oder Ausland beantragt; die eingereichte Dissertation oder Teile von ihr wurden nicht für ein anderes Promotionsvorhaben verwendet. Mir ist bekannt, dass unrichtige Angaben die Zulassung zur Promotion ausschließen bzw. später zum Verfahrensabbruch oder zur Rücknahme des erlangten Grades führen.

(Ort)....., den .....

(Unterschrift)

Index

1 | Introduction

1.1 | Summary & Motivation

A constant challenge for the insect's nervous system is the omnipresence of diverse stimuli. These external cues trigger the organisms behavioural patterns to alternating environmental conditions. Therefore insects are endowed with specialized sense organs. These sensory neurons respond adequately to specific stimulation, as specific behaviour is only evoked by specific sensory stimuli.

The basis for specific behavioural patterns of insects is modulated by the senses of photoreception, proprioreception, chemoreception, thermosensation, touch and hearing. In *Drosophila*, specific sounds entail courtship **(Spieth et al., 1952, Shorey et al., 1962, Narda et al., 1966)**. It is ascertained that *Drosophila* does hear with its antennae via scolopidia, which are arranged in a chordotonal organ called Johnston´s Organ (JO) **(Johnston 1855; Boekhoff-Falk G et al., 2005; Yack et al., 2004)**. The JO in the antenna is the largest chordotonal organ in *Drosophila* followed by the femoral chordotonal organ (FCO) in the leg of *Drosophila*. Insect legs are endowed with mechanoreceptors, the femoral chordotonal organs (FCOs) **(Göpfert et al., 2005; Nishino et al., 2003; Field et al., 1998; Büschges et al., 1994)**, that detect angular changes between the femur and the tibia. In *Drosophila*, little is known about the function of the FCO **(Shanbhag et al., 1992)**.

Here I show that functional properties of the *Drosophila* FCO can be dissected by use of the Gal4-UAS system in combination with transcuticular *in vivo* Calcium imaging. As sinusoidal stimulation at relative small stimulus amplitudes elicited changes in intracellular ionic calcium (Ca^{2+}) concentration in the FCO, the effect of substrate vibration on *Drosophila* walking behaviour was proposed. But lately developed fly tracking software for high-throughput ethomics **(Branson et al., 2009)** showed that substrate vibrations have no specific effect on *Drosophila* walking behaviour. Instead present evidence suggests that *Drosophila* compensates for substrate vibration by detection via the FCO and therefore is able to control its body posture. A modification of

transcuticular *in vivo* Calcium imaging was used to locate the neuronal activity region of Inactive, a protein involved in *Drosophila* hearing and a mechanotransduction channel candidate. I could show that *inactive* mutants still respond to sound like stimulation with ciliary calcium currents.

1.2 | Sensory Neurons of Insects

The peripheral nervous system of insects comprises two major classes of sensory organs: Type I neurons are monodendritic and ciliated, bearing a single ciliated dendrite **(Tracey et al., 2003)**, whereas type II neurons are multidendritic neurons (MD) whose dendrites form no ciliar structures **(Keil et al., 1997)**.

Type I organs are further subclassified into photoreceptors, external sensory organs (ES) (involving gustatoric, olfactoric neurons and mechanoreceptive sensilla like bristle and campaniform sensilla) and mechanosensitive chordotonal organs (CHO) **(Kernan et al., 2007)**. These types of sensory neurons specialize from sensory organ precursor cells (SOP) **(Jan & Jan, 1994)**. The specialization of the SOP cells is defined by proneuronal genes of the *achaete-scute* complex and *atonal*. ES and MD neurons develop from solitary precursor cells by transcription factors of the *achaete-scute* complex, whereas photoreceptors and CHOs develop from clusters of SOP cells by the gene *atonal*. *Drosophila* mutant for the gene *atonal* totally lack CHO's and show disrupted eye development **(Jarman, 1995)**, which highlights the eminent function of atonal in sense organ development **(Kernan 2007)** (FIG1.2).

1.2.1 | External Sense Organs

The ciliated Type I ES sensory units are composed of four specialized cell types: one to several bipolar neurons and three different accessory cell types: trichogen (attachment cell), thecogen (sheath cell) and tormogen (socket cell). The trichogen cell forms the cuticular hair of tactile hair bristles or the analogous structures of the cap in campaniform sensilla or the scolops of chordotonal organs. Mechanical forces deflect this structures. The leverage of these structures is transmitted via the dendritic cap on

to the dendrites of the actual neurons. The dendritic cap, an extracellular structure of the trichogen cell is attached to the distal part of the sensory neurons dendrite. The dendrite is segmented into the proximal "inner segment" and the distal "outer segment". The "outer segment" is a modified stereocilium with an $9 \times 2 + 0$ arrangement of microtubule in the axoneme **(McIver et al., 1985)**. The "outer segment" is floating in an endolymph filled space formed by the trichogen and tormogen cell. High K^+ and low Ca^{2+} concentration are characteristic for the endolymph of Type I neurons **(Grünert und Gnatzy, 1987)**. The tormogen cell forms a cuticular joint with the trichogen cell. The thecogen cell sheaths the neurons soma and most of the dendrites "inner segment". These cell types form the stimulus receiving structures around the dendritic part of the neuron **(Field et al., 1998, Bang et al., 1992)**.

1.2.2 | Chordotonal Organs

Chordotonal Organs are internal stretch receptor organs that, monitoring relative movements between body parts, primarily serve proprioreception. The organ is usually attached to the cuticle and connected to the hypodermis, often by a special ligament. In adult flies chordotonal organs routinely bridge the joint between two limb segments **(Field et al., 1998)**.

Chordotonal Organs are composed of multicellular units called scolopida, which feature an analogous organisation and composition as ES organs. Each scolopidium consists of three supporting cells (a cap cell, the scolopale cell and a ligament cell) and one (monodynal scolopidia) to four (heterodynal scolopidia) neurons. The eponymous structure for the scolopidium is the scolops. The scolops, scolopale tube or dendritic cap is secreted by the trichogen or attachment cell and connects the distal part of the dendritic cilium with force receiving extracellular structures.

Scolopidia can be subclassified by distinct cap structures according to their connection with the cilium. The cilium of amphinematic scolopidia (JO) is enclosed and loosely attached by an electron dense scolopale tube that extends into a thread that can be either connected to the cuticle or to sub-epidermal structures. In monenematic scolopidia (FCO) the cilium is surrounded by the dendritic cap and is attached to it

(Graber et al., 1882, McIver et al., 1985, Yack et al., 2004, Eberl et al., 2007).

The neurons are bipolar and monodendritic, bearing a proximal axon and one distal dendrite each. The neurons are supported apically by the cap cell and proximally by the ligament cell. The dendrite is subdivided into an inner and an outer segment, with the latter representing a primary cilium with a 9x2+0 axoneme (nine outer microtubule doublets ("9x2") and no central microtubules ("+0")). This structure is anchored via the basal bodies to ciliary rootlets in the inner segment **(McIver et al., 1985)** (see FIG 1.1). The *Drosophila* neurons of the JO and the FCO show a swelling at the outer segment. This ciliary dilation is always characterised by the presence of electron-dense material in its centre **(Field et al., 1998)**. Another characteristic of the dilation is a clear connection between each microtubule doublet and the ciliary membrane **(Field et al., 1998)**.

The whole cilium is enclosed by the scolopale cell, giving room to a scolopale space at the outer segment. The scolopale cell tightly encloses the dendritic "inner segment" and attaches to it by desmosomes on the inner surface of each scolopale rod. The scolopale rods are actin rich and support the scolopale space arround the dendritic "outer segment".

This space is filled with an endolymph assumed to contain similar high K^+ and low Ca^{2+} concentration as in other type I neurons **(Grünert und Gnatzy, 1987)**. Proximally the scolopidium is connected by the ligament cell to extracellular structures such as the hypodermis **(Snodgrass 1926, Young et al., 1970, Chu-Wang et al., 1972, Zacharuk et al., 1978, Altner et al., 1984, Mclver et al., 1985)**. The scolopidia layout, composed of extracellular scaffolds, intercellular junctions, cyto skeletal and ciliary structures, facilitates the transduction of mechanical forces (see FIG 1.1).

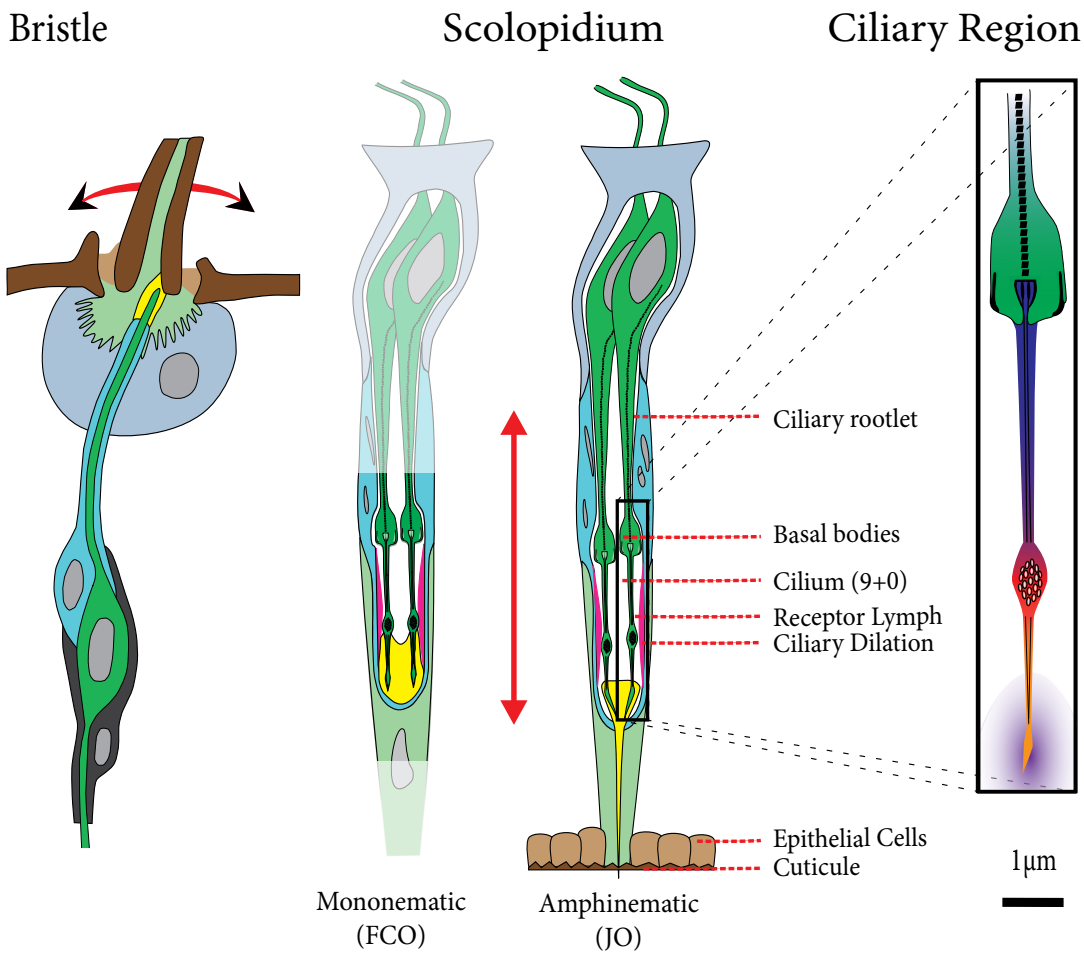

FIG 1.1 | Insect Mechano Sensory Neurons

Scolipidium

- Sensory Neurons
- Tormogen | Socket | Ligament Cell
- Thecogen | Sheath | Scolopale Cell
- Trichogen | Attachment Cell
- Glial Cell
- Epithelial Cells

Asscociated Structures

- Scolopale rods
- CAP
- Cuticule

Proteins involved in Mechanotransduction

- NAN / IAV
- DCX-EMAP
- NOMPC

→ Direction of Mechanical Forces

Several proteins are known to locate to the distal part of the scolopidium:
The TRPV's NAN & IAV, which form a heteromultimeric channel and NOMPC, a TRP channel, are essential for *Drosophila* auditory transduction. DCX-EMAP carrying two doublecortin domains is likely to be required for mechanotransduction and amplification as well.
TRP(V): Transient Receptor Potential (Vanilloid) Channel
EMAP: Echinoderm Microtubule Associated Proteins

[Modified from: Shigekazu UG 1965, Field& Mattheson 1998, Walker et al 2000, Yack et al 2004, Eberl et al 2007, Bechstedt et al 2010, Cheng, 2010; Liang , 2010]

1.3 | The *Drosophila* Femoral Chordotonal Organ

1.3.1 | Morphology of the Femoral Chordotonal Organ

The *Drosophila* adult leg houses the relative small tibial chordotonal organ (TCO) and the FCO. The FCO is located dorso-rostral proximal in the femur with a length of ~ 175µm (FIG. 1.2| a)). The FCO consists of about 74 mononematic scolopidia arranged in three morphological distinct subgroups **(Shanbhag et al., 1992)**. During my diploma thesis I could show that certain Gal4 - driver lines **(F-Gal4 & NP0761; Wiek, 2009; Kamikouchi et al., 2006 ; chapter 2.1.5)** expressed in the JO also label the FCO. Confocal imaging of flies expressing GFP under control of NP0761 in the FCO and image processing with Amira revealed that the FCO consists of 134 Neurons. Three subgroups could be morphologically distinguished by the arrangement and number of their neurons (FIG. 1.2| b)).

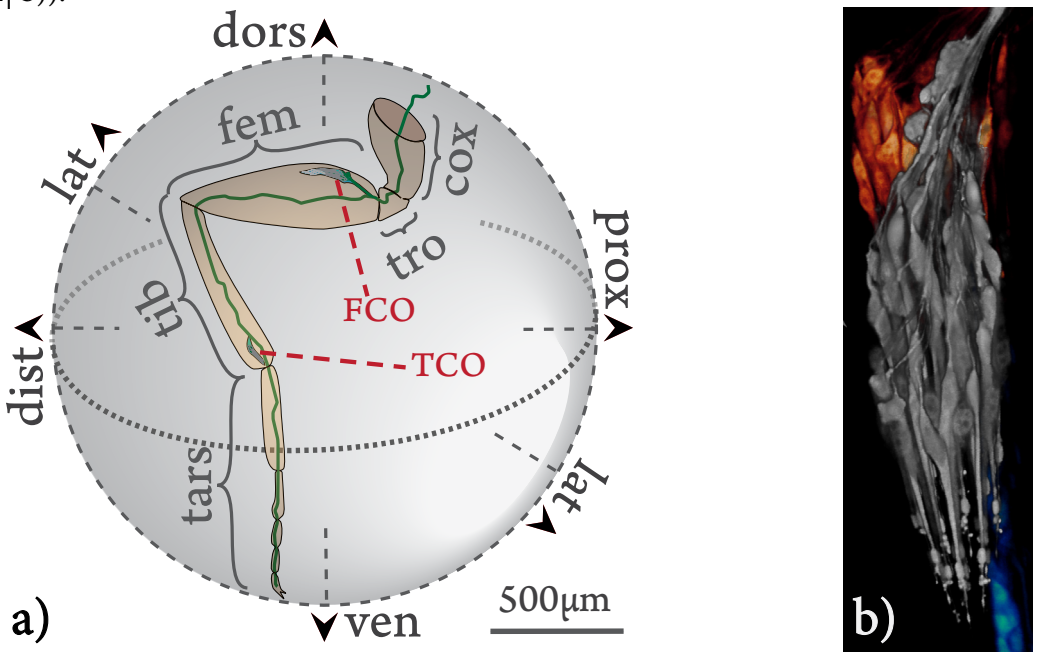

FIG 1.2 | The *Drosophila* FCO
a) Sketch of the leg with FCO and TCO (3D Cursors showing orientation and position of the FCO) [modified from Shanbag (1992)]
b) FCO amira®4 3D reconstructions of +/+;UAS-Cam2.1; NP0761flies
subgroups colour code: I grey ≈ 64 neurons; II red ≈ 42 neurons; III blue ≈ 28 neurons
Shanbhag et al proposes that the largest subgroup (I) is attached to the cuticule at the femur tibia joint and that the two smaller groups (II+III) insert onto muscles. [modified from Wiek, 2008]

Observation of the **FCO** revealed that its axons run into a structure called glomerulus. Shanbhag **(1992)** observed by electron microscopy that all FCO axons run into the glomerulus and form synapses connecting between each other. Consistent with this observation, immunostaining with 3C11 antibody (anti SYNORF 1), which detects synapsin **(Klagges et al.,1996)**, and the reporter fusion construct UAS-nsyb::GFP, which locates to presynapses **(Ito et al., 1998)**, both label the glomerulus (FIG 1.3).

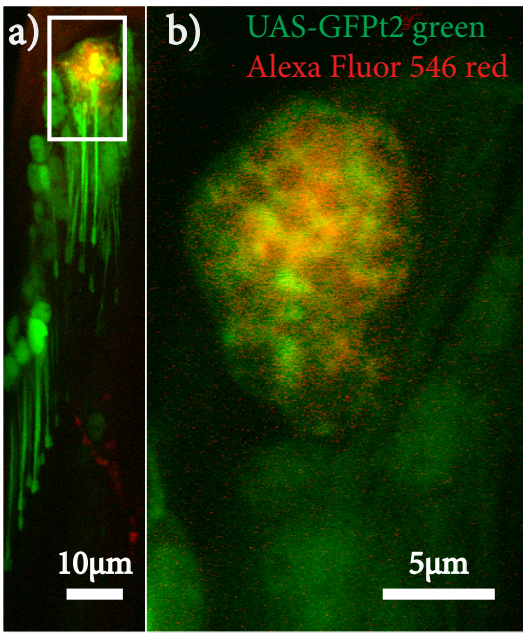

FIG 1.3 | Glomerulus

FCO and Glomerulus 3C11-Antibody Staining (Alexa Fluor® 546) of UAS-GFPT2;NP0761 Confocal Image of Leg Whole -Mount. a) FCO overview b) Glomerulus [modified from Wiek 2008]

The afferent nature of the glomerulus was proven by the fact that synaptobrevin expression was driven by a chordotonal organ specific driver line. In *atonal* hemizygous mutant flies, in which no chordotonal organs are present, Antibody 3C11 does not label any peripheral synapses.

Peripheral synapses as in the glomerulus are rarely described in insects. Afferent peripheral synapses are only found between inter-and moto-neurons of spiders (**Foelix et al., 1975; Hayes et al., 1982; Rajashekhar et al., 1989; Igelmund et al., 1991**) and efferent peripheral synapses are described for the *Arachnid Cupenius salei* **(Fine et al., 1999)** and the chelicerate *Limulus* **(Fahrenbach et al., 1975; Hartline et al., 1972)**. In *Limulus* peripheral synapses increase contrast in vision by lateral inhibition. Serial and reciprocal synapses of glomerular or neuropile structures are said to be the basis for presynaptic inhibition**(Bullock et al., 1977)**. Except for the glomerulus, the only other efferent synapses described in *Drosophila* are between inter- and moto- neurons **(King and Wyman, 1980)**. Shanbhag **(1992)** proposes that the glomerulus in the *Drosophila* leg is integrating and preprocessing sensory information of the FCO. While the morphology of the FCO could be revealed by these techniques, its function remains unclear.

1.3.2 | Function of the Femoral Chordotonal Organ

The coordination of movement depends on the interplay of internal cues of the central nervous system (CNS), muscles and information of the peripheral nervous system (PNS). So called central pattern generators (CPG) generate the rhythms of movement. The CPGs rhythms are triggered and altered by intrinsic and extrinsic input of the PNS's sensory neurons **(Pearson et al., 1995; Orlovsky et al., 1999; Büschges et al., 2005)**. In stick insect walking the transition between swing and stem phase are modulated by mechanosensory organs in the legs.

Next to bristle hair fields and campaniform sensilla, the FCO of the stick insect *Cunicuilina impigria* is mainly responsible for feedback control of the femur tibia joint posture, which is a hinge joint **(Kernan et al., 1994; Bässler et al., 1988; Burrows et al., 1996; Zill et al., 2004)**. The position of the tibia relative to the femur is sensed by the FCO. The FCO's general function is described as monitoring the position, angular velocity and acceleration of the tibia **(Hofmann et al., 1985 & 1985; Büschges et al., 1994; Nishino et al., 2003)**. The joint movement is controlled by the extensor and flexor tibia muscle **(Bässler et al., 1993)**.

Apart from its well-established role in proprioception, an involvement of the FCO in vibration sensing has been proposed **(Kernan et al., 2007)**. CHO in *Orthopterans* and *Hemipterans* detect substrate vibrations **(Field et al., 1998)**. In *Orthopterans* the leg scolopidial tympanal organ functions as an ear. In *Drosophila* it is not known if the FCO is detecting intrinsic signals such as changes of position, angular velocity and acceleration of the tibia or if it detects extrinsic signals such as airborne or substrate-borne vibrations. It is known that airborne and substrate vibrations have an effect on *Drosophila* walking behaviour. Fabre et al. **(2012)** show that substrate vibrations affect *Drosophila* walking behaviour, as female flies stops walking due to substrate vibrations generated by male shaking their abdomen during courtship. They suggest that in *Drosophila* tremulations of the abdomen are transmitted via the male legs and that females perceive the substrate vibrations carried through the legs **(Fabre et al., 2012)**.
Lehnert **(2013)** shows that walking behaviour is altered by airborne vibrations (low intensity sound at 300 Hz) and that the *Drosophila* JO is essential for the behavioural response **(Lehnert et al., 2013)**.

1.4 | *Drosophila* Hearing

1.4.1 | The Johnston`s Organ

Drosophila mating success does not only rely on olfactory and visual cues but also on sound perception **(Göpfert et al., 2002)**. During courtship the male fly, in close proximity to a female, extends one of its wings and vibrates it emitting species-specificsounds called courtship songs **(Schilcher et al., 1976; Hoy et al., 1988; Hall et al., 1994)**. The two discriminable types of courtship songs, sine **(Schilcher et al., 1976)** and pulse songs **(Ewing et al., 1968)**, are dominated in the range of 150 to 200 Hz. *Drosophila* senses sound as particle velocity that acts on its antenna. The antenna consists of three segments. The scapus, the 1st antennal segment and part of the antenna that comprises muscles, enables the fly to orientate the antenna. The pedicelus, the 2nd segment, houses the auditory organ, the Johnston's organ (JO) **(Johnston et al., 1855; Boekhoff-Falk et al., 2005; Yack et al., 2004)**. The funiculus, the 3rd antennal segment, is the sound perceiving structure **(Göpfert et al., 2001)**. It bears the arista, a feather-like appendage which functions together with the funiculus as a sound receiver **(Göpfert et al., 2002)**. The funiculus, rotating due to sound particle velocity, is anchored via a hook in the pedicelus. The 3rd segment's hook connects to the scolopidial attachment cells of the JO. The JO, a chordotonal organ, is formed by approximately 227 of these amphinematic scolopidia **(Kamikouchi et al., 2006)**. Only 10-15% of the JO scolopidia hold three and the rest two sensory neurons **(Todi et al., 2004; Caldwell et al., 2002)**.

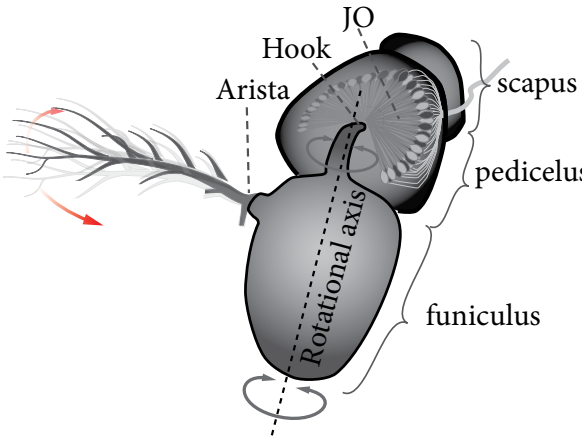

FIG 1.4 | *Drosophila* Antenna
A1 | 1st segment: scapus; A2 | 2nd segment pedicelus; A3 | 3rd segment: funiclus
In response to sound the 3rd segment rotates along its longitudinal axis. This rotational force is passed onto the JO, located in the 2nd segment, by the 3rd segment's hook, thereby stretching and compressing the scolopidia. The antenna can be actively positioned by the 1st segment the only segment endowed with muscles. → rotational axis

1.4.2 | Auditory Transduction in *Drosophila*

The sound receiver, the 3rd segment and its arista, rotate back and forth as a rigid body when stimulated by sound. The hook couples this movement into stretch and compression of JO scolopida, which are arranged in two opposing groups around the hook, which leads to opening and closing of mechanically gated ion channels. These channels transduce the applied mechanical force into changes of the membrane potential **(Albert et al., 2007; Nadrowski et al., 2009)**.

The sensitivity of the *Drosophila* antennae is achieved by the organ's structure and intrinsic processes of the JO. The JO neurons actively generate motions that nonlinearly amplify the sound-induced antennal vibration when the sound intensity is low **(Göpfert et al., 2006)**. This amplification is frequency-specific, maximally enhancing vibrations at the antenna's mechanical best frequency.

Two different approaches were used to examine the intrinsic processes of mechanotransduction in *Drosophila* hearing **(Göpfert et al., 2002)**. One was to analyse the transducer mechanics by monitoring the arista displacement, the other was to record antennal nerve responses (see FIG 1.5).

Until now several proteins are known to affect *Drosophila* hearing **(Senthilan et al., 2012)**, although it still remains unclear which channel or protein complex is the primary transducer. Candidate transdution channels for hearing in *Drosophila* are NOMPC (No mechano receptor potential C; also called TRPN1) and the proteins of the heteromultimeric TRPV channel formed by Nanchung & Inactive (NAN/IAV).

They belong to the transient receptor potential (TRP) superfamily of ion channel families. TRP channel functions are implicated in a variety of sensory processes **(Ernstrom et al., 2002; Tracey et al., 2003 ;Voets et al., 2005; Rosenzweig et al., 2005; Xu et al., 2006; Liu et al., 2007; Damann et al., 2008)**. The TRP superfamily comprises several subgroups: TRPA (ANKYRIN), TRPC (CANONICAL), TRPM (MELASTATIN),TRPML (MUCOLIPIN), TRPN (NOMPC), TRPP (POLYCYSTIN), TRPV (VANILLOID) **(Montel et al., 2002)**.

All members of this superfamily are cation permeable, share some sequence homology and show 6 transmembrane domains, predicted by their DNA sequence. Members of these channel families are also found in vertebrate auditory hair cells **(Göpfert et al., 2006)**.

Several findings suggest that NOMPC is the transduction channel:

First, NOMPC is required for mechanical amplification by JO neurons, as mutants do not show feedback amplification (see FIG 1.5 | a) **(Göpfert et al., 2006)**. This requirement may reflect a role in transduction as amplification is mechanistically linked to transduction and requires information about the intensity, frequency, and phase of the incoming sound **(Nadrowski et al., 2008)**. By contrast, NAN/IAV reportedly facilitate amplification, suggesting that transduction continues in the absence of TRPVs (see FIG 1.5 | a). The nerve response of the mutants on the other hand show that *iav* mutants do not elicit any measurable potentials whereas *nompC* mutants shows reduced sound evoked potentials (see FIG 1.5 | b) **(Göpfert et al., 2006)**.

Second, NOMPC is distinct to the other TRP channels by a special structural feature, its N-terminal ankyrin repeats. In NOMPC 29 ankyrins form one turm of a functional spring **(Howard et al., 2004; Liang et al., 2011)**. The predicted gating spring stiffness of hair cell transduction channels matches the stiffness of this spring **(Howard et al., 2004; Lee et al., 2006; Sotomayor et al, 2005)**.

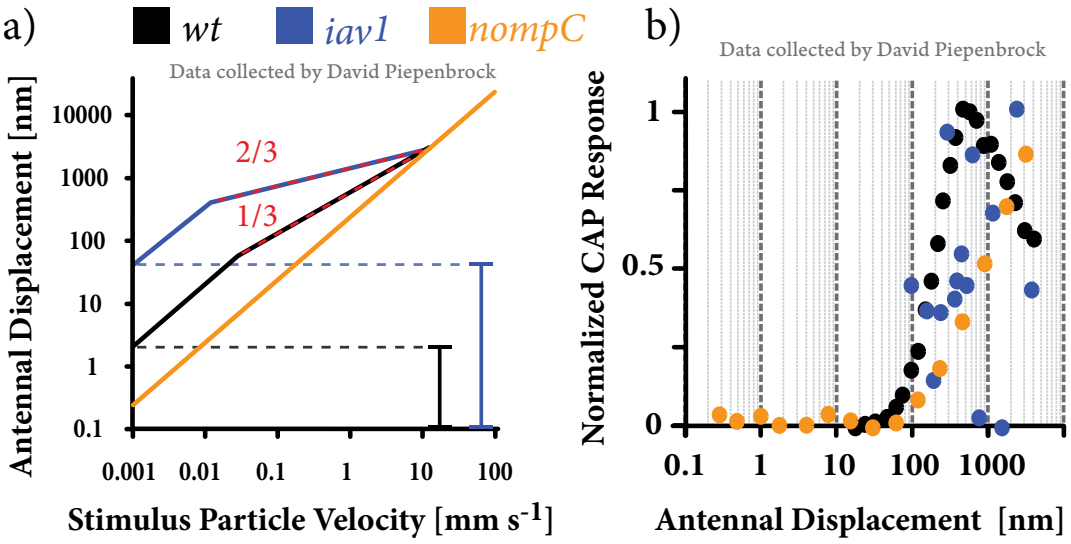

FIG 1.5 | Antennal Response Characteristics

a)Nonlinear amplification: Log-log coordinates of the displacement of the fly's antennal sound receiver as a function of the stimulus particle velocity. Displacements and particle velocities are given as Fourier amplitudes at the stimulus frequency, which was adjusted to the individual best frequency of each receiver. Red lines, nonlinear regimes; marker, gain in sensitivity due to nonlinear amplification.

b) Nerve response: Normalized compound action potential plotted against log scaled antennal displacement. The stimulus was played at the antenna best frequency. The best frequency maximum nerve response is at ~ 1000nm stimulus amplitude. [modified from data of David Piepenbrock and Göpfert et al., 2006]

A proposed model of TRP-channel function by these findings is that NOMPC is an auditory transducer, required for feedback amplification, which is negatively controlled by NAN/IAV. As loss of NOMPC reduces but does not totally abolish sound evoked potentials, additional transduction channels "X" must exist **(Göpfert et al., 2006; Lu et al., 2009)** (see FIG 1.6). This model is in consistency with the localisation of the afore mentioned channels. In the JO NOMPC is located at the most distal part of the scolopidial cilium that is directly attached to the sound receiver **(Cheng et al., 2010 ; Lee et al., 2010; Liang et al., 2011)** (see FIG 1.1 & FIG 1.6).

NAN/IAV on the other hand is located proximal to NOMPC between the ciliary dilation and the basal body **(Gong et al., 2004; Bechstedt et al., 2010; Cheng et al., 2010; Liang et al., 2010)** (see FIG 1.1 & FIG 1.6). The model is further underlined by the fact that ablation of the sound receptors leads to the same effects ensued from mutations in *nompC*. The residual nerve responses in sound receptor ablated and *nompC* mutants flies match each other. In addition ablation of the gravity wind receptors has no effect on active amplification and the nerve response resembles those of wild-type flies **(Effertz, Wiek & Göpfert, 2011)**.

Transcuticular Ca^{2+} imaging **(Kamikouchi et al., 2009; Kamikouchi & Wiek et al., 2010)** revealed that gravity wind receptors are responsible for the remaining nerve potential of *nompC* mutants and that *nompC* mutant flies show no Ca^{2+} response in sound receptors **(Effertz, Wiek & Göpfert, 2011)**.

A recent study modifies this model for auditory transduction suggesting that NOMPC, through active amplification processes, rather modulates than mediates transduction in auditory receptor cells **(Lehnert et al., 2013)**. Lehnert et al propose that NAN/IAV are components of the transduction complex **(Lehnert et al., 2013)**. Their modification of the model is based on non-invasive recordings of giant fibre neurons, as neuronal signals generated by auditory receptor neurons are propagated through gap junctions to giant fibre neurons. Hereby they show that signals are not propagated in iav^{1} and nan^{36a} mutants and that $nompC^{3}/nompC^{1}$ mutant fly show decreased sensitivity of generator currents to antennal rotations but on the other hand adaptation to static forces is not prevented. By the latency and speed of the generator currents recorded they imply that NAN/IAV is directly gated by mechanical force, as proposed amplification **(Göpfert et**

al., 2006; Kamikouchi et al., 2009; Lee, 2010) through second messengers for NAN/IAV would occur in microseconds. They further underline this by the fact that NAN/IAV does not colocalize with NOMPC in the JO dendrite ruling out direct protein-protein interactions between these components.

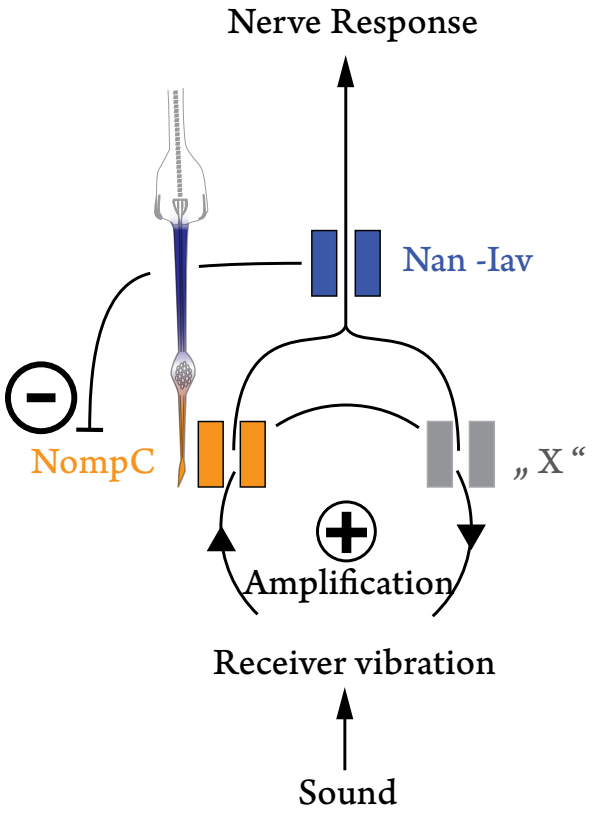

FIG 1.6 | Model of TRP-channel function in the *Drosophila* ear.

NOMPC may be an auditory transduction channel, as loss of these channels abolishes active amplification. Additional transduction channels "X" must exist, as reduced but not totally abolished sound evoked antennal nerve potentials are recorded in flies lacking NOMPC. The NAN/Iav heteromultimeric channel acts downstream of NOMPC and negatively controls amplification in a NOMPC dependent way. Loss of this control leads to excess amplification, resulting in self - sustained oscillations of the receiver. As judged from the complete loss of nerve potentials in *nan* and *iav* mutants, NAN/Iav is additionally required for propagating electrical signals from the transduction site to the antennal nerve.

[modified from Göpfert et al. (2006) & Lu et al (2009)]

1.5 | Ca^{2+} Imaging

1.5.1 | Ca^{2+} Imaging as a Means of Monitoring Neuronal Activity

Neuronal activity comprises various processes that are associated with the excitation of neurons such as calcium influx, altered metabolism rates, release of synaptic vesicles or most prominently changes in the membrane potential. To investigate the activity characteristics of neurons extra- and intra cellular recording techniques and combinations of these are widely used. Drawbacks of these techniques are constraints in spatial resolution, as for instance with extracellular recordings, whereas intracellular recordings are limited to one to several cells. Other major disadvantages are the integrity as well as the neuronal size.

The model organism *Drosophila melanogaster* is an example in which typical recording techniques reach their limits. For example, to record from chordotonal organs, the cuticula and the suporting cells of the scolopidial organ have to be harmed. This would probably lead to no true response, as CHOs depend on the integrity of their supporting cells and the cuticle to which they are connected **(Kamikouchi & Wiek et al., 2010)**. A solution for the above mentioned constraints is the visualisation of neuronal activity by special sensors. Voltage gated sensors such as genetically-encoded voltage indicators (GEVIs) can be used. But only recently their drawback for signal to noise ratio has been solved **(Kralj et al., 2012)**.

Ca^{2+} imaging has been proved to be a solid technique **(Berridge et al., 1998; Grienberger et al., 2012)**. Calcium is a key player in regulating neuronal processes. Changes in Ca^{2+} concentration lead to neurotransmitter release or alter the excitability of neurons. Ca^{2+} can be either released from internal stores like the endoplasmatic reticulum or it can influx through voltage, receptor and mechanic gated ion channels **(Berridge et al., 1998; Montell, 2005)**. Different genetically encoded Ca^{2+} indicators (GECI) are used to monitor neuronal activity in *Drosophila melanogaster*. For instance Cameleon 2.1 (Cam 2.1), a ratiomeric calcium sensor, was used to investigate the function of JO sub populations (see chapters 2.1.1, 2.2.1 & 3.1) through expression of driver lines that labelled distinct

auditory sensory projections of the JO **(Kamikouchi et al., 2006)**. One sub population could be identified as sound sensitive (AB neurons) and the other as gravity/wind sensitive (CE neurons) **(Kamikouchi et al., 2009)**.

1.5.2 | Ca^{2+} Indicator Cameleon 2.1

Cameleon 2.1 (Cam2.1) is a genetically encoded Ca^{2+} indicator (GECI). It bears the fluorescent proteins enhaced Cyan Fluorescent Protein (eCFP) and the enhanced Yellow Fluorescent Protein (eYFP) that are genetically modified versions of the Green Fluorescent Protein (GFP), which is a native protein derived from the jellyfish *Aequorea victoria*. GFP has a barrel shaped structure composed of 238 amino acids. It has a major excitation peak at 395 nm and an emission peak at 509 nm (Chalfie et al., 1994). From N- to C-Terminus the fusion protein Cam2.1 consists of mutant eCFP, a Ca^{2+} binding domain of calmodulin (Cam), the calmodulin-binding peptide M13 and eYFP (see FIG 2.4| c). Binding of up to 4 Ca^{2+} molecules to Cam leads to enclosing of the M13 domain (see FIG 2.4| b-d). This conformational change brings the two fluorescent proteins in close proximity for Förster Resonance Energy Transfer (FRET) **(Miyawaki et al., 1997 & 1999)**. FRET occurs when two fluorescent dyes are in the Förster radius of 0.5-10 nm and have overlapping emission and excitation wavelength (see FIG 2.4| a). The so called donor (eCFP) is then directly transferring energy, without photon emission, to the acceptor (eYFP). In the case of Cam2.1 the excitation wavelength of eCFP is 440 nm and the emission wavelength is 476nm, which is near the eYFP peak excitation wavelength of 480 nm. When Cam2.1 is excited at 440nm, in the absence of calcium the eCFP emission wavelength of ca. 480 nm is dominant. When the Ca^{2+} concentration rises the binding of calcium leads to a conformational change reducing the eCFP and eYFP distance allowing FRET. This shifts the dominant emission wavelength to ca. 540 nm (see FIG 2.4| b-c). Therefore Cam2.1 is an ideal ratiomeric sensor to measure changes in Ca^{2+} concentration. The transgenic construct of UAS-Cam2.1 allows the expression in *Drosophila melanogaster* where it is used as a sensor of neuronal activity **(Kamikouchi & Wiek RJ et al., 2010; Fiala A et al., 2002 & 2003; Effertz T, Wiek RJ, Göpfert MC, 2011)**.

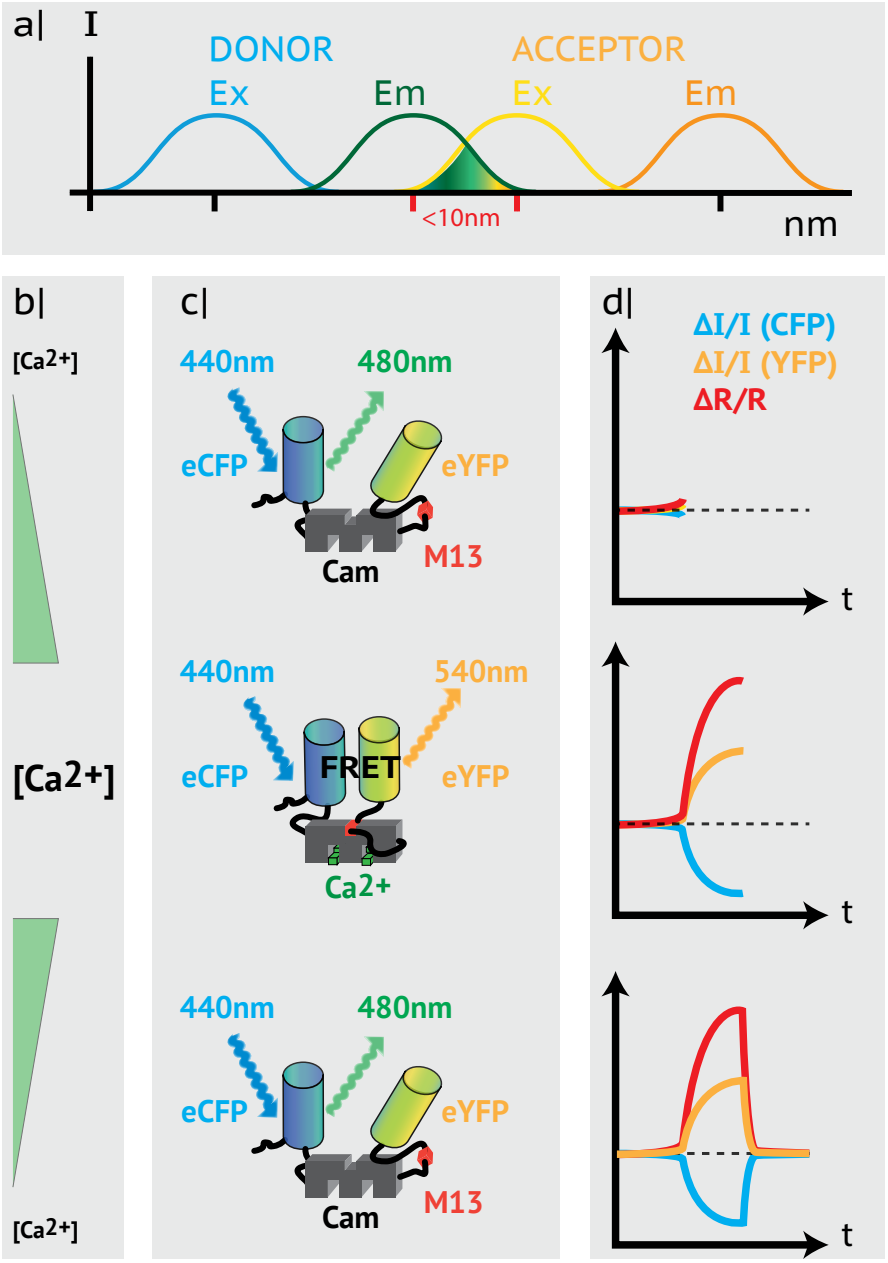

FIG 2.4 | Cameleon 2.1

Cameleon 2.1 is a calcium dependent FRET sensor. It consists of eCFP and eYFP linked by Cam and M13. In absence of calcium the eCFP emission wavelength of ca. 480nm is dominant. Binding of calcium leads to a conformational change reducing the eCFP and eYFP distance. As a result Förster resonance energy transfer occurs and shifts the dominant emission wavelength to ca. 540nm.
a| Scheme of Förster radius 0.5-10 nm; b| change in Ca^{2+} concentration; c| Scheme of Cam2.1 changing its conformation of binding up to four Ca^{2+}-Ions; d| Shift of eCFP and eYFP intensities and ratio over time according to Cam2.1 conformation, corrected for bleaching.

[modified from Riemensperger T et al. (2012)]

2 | Material & Methods

2.1 | *Drosophila melanogaster* & Genetic tools

2.1.1 | The Model Organism *Drosophila melanogaster*

Flies are often used for biological studies due to their fast reproduction cycles and, connected to this, low maintenance costs.

The fruit fly *Drosophila melanogaster* is one of the oldest and best studied model organisms, described as early as 1830 by Johann Wilhelm Meigen **(Meigen, 1830)**. In 1901 first used as a model organism by William Ernest Castle it only took nine years until Thomas Hunt Morgan started his fundamental works on the structure of *Drosophila* Chromosomes **(Castle et al., 1906; Morgan, 1913)**. His chromosome theory of inheritance underlined the just rediscovered work of Mendel and became the fundament of classical Genetics. With over 700 hundred other fruitfly species *Drosophila melanogaster* belongs to the family of *Drosophilidae*. The whole genome is sequenced since 2000 **(Adams et al., 2000)**. Of the 13.600 genes discovered, a huge number shares not only sequence homology with human and vertebrate genes, but has also the same function.

For example the *Drosophila melanogaster* gene *atonal* fully rescues the phenotype of *Math1* (mouse atonal homologue 1) null mice, which are shown to die shortly after birth **(Wang et al., 2002)**. Nowadays several genetic tools, like the GAL4/UAS **(Brand & Perrimon, 1993)** system, help to manipulate gene expression in *Drosophila melanogaster*. For example the use of randomly created GAL4 driver lines helped to visualize and cartograph different subpopulations in the JO and its corresponding projection areas in the *Drosophila* brain **(Yoshihara and Ito, 2000; Kamikouchi et al., 2006)**. Due to this relatively easy genetic accessibility of the *Drosophila melanogaster* genome, studies combining the physiological properties, like response and tuning of mechanosensoric cells, with genetic screens help to understand the evolution, development, function and pathology of mechanoreceptors like hair cells in *Homo sapiens* **(Senthilan et al., 2012)**.

2.1.2 | Fly Husbandry

Fly stocks were kept in cylindric plastic vials of 64 mm height and 26 mm width **(FIG 2.1; greiner bio-one:PS TUBE flat bottom)**. These vials were enclosed with foamy ceapren mite protection plugs **(greiner bio-one: Kat.-Nr. 205 101)**. These vials are filled up to a quarter with the nutrition medium (see 2.1.3) on which the female fly also deposits its eggs. For new crosses at least 3 virgin females and 2 males of different genotype were collected under CO_2 - anaesthesia and placed into the nutrition bottled vials. The flies were kept at two different temperatures. At least three copies of every stock line, at different stages, were kept at 18°C to create a slower generation period of about 14-20 days in contrast to flies kept at 25°C. Crosses and weak fly stocks were kept at 25°C with an average reproduction cycle of 9-10 days, as 25 °C is the healthiest temperature for flies **(Greenspan, 2004)**. The humidity at both temperatures was levelled to 60% and the day and night cycle was 12h :12 h. Stocks were switched to new vials ca. every three weeks.

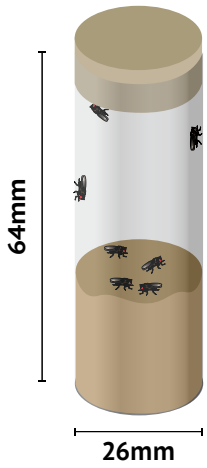

FIG 2.1 | Fly Vial

2.1.3 | Nutrition Recipe

125g agar was soaked in 10 litre of water and cooked over night. On the next day soy bean flour, yeast, maize meal, treacle and malzin were separately mixed and dissolved (see chart 2.1). These ingredients were mixed into the agar and the whole mixture was cooled down under constant stirring for 1h until 55°C were reached. Then the fungicide propionic acidand the bactericide Nipagin (15% in 70 % Ethanol) were stirred in. The fly vials were then filled to a fourth with the still hot fluid medium.

chart 2.1 | Nutrition Ingredients

125 g	agar	soak over night
100 g	soy bean flour	dissolve in 1litre H2O
180 g	yeast	
800 g	maize meal	dissolve in 2litre H2O
220 g	treacle	dissolve in 1litre H2O
800 g	malzin	dissolve in 1litre H2O
63 ml	propionic acid	
15 g	Nipagin	dissolve in 50 ml EtOH

2.1.4 | Transposable Elements: P- Elements, PiggyBac, Minos

A transposable element or transposon is a small DNA segment which is able to change its genomic position, by jumping through the genome and generating mutations. A distinction is drawn between RNA (Retoransposons / Class-I-transposons) and DNA dependent transposons (DNA-transposon / Class-II-transposons).

Retrotransposons transcribe their code from DNA to RNA. Reverse transcriptase, often coded by the retrotransposon itself, creates a DNA copy from the RNA, which is then inserted at a new position in the genome ("Copy & Paste").

DNA transposons, on the other hand, do not depend on an RNA agent, their transposition depends on the enzyme transposase ("Cut & Paste"). There are autonomous transposons, encoding for the transposase itself, and non-autonomous transposons that either have deletions in the transposase gene or miss it.

Today it is possible to choose between different transposons for targeted and untargeted manipulations of the genome. The most common transposon in *Drosophila* genetics are the P-Elements, followed by PiggyBac and Minos elements.
P-Elements have been described in the 1970's in a comparison of wild-type (*wt*) *Drosophila* melanogaster strains and strains held under laboratory conditions since 1905 **(Kidwell et al., 1977)**. As only *wt* strains carried P-Elements, they must have entered the *Drosophila* melanogaster genome posterior to the isolation of laboratory strains **(Ryder E & Russell S, 2003)**.

The autonomous *wt* P-Element, flanked by terminal inverse repeats, is cut out at these repeats by P transposase, forming sticky ends. The palindromic sticky ends are fused by the P transposase, forming a circular double strand of genomic DNA. As the excision process is imprecise to a certain level, DNA flanking the P-Element can be co-excised as well, causing deletions of the host genome. The circular form is "pasted" by the P transposase at another genomic region (see FIG 2.2). In somatic cells P transposase is not transcribed, as a splicing event is inhibited, so that only germ line cells express P transposase **(Amarasinghe et al., 2001)**. Female *wt* strains carrying the P-Element express an inhibitor of P transposase, so that P-Element mobility is restricted to *wt* females **(Ryder E & Russell S, 2003)**. To use P-Elements as a genetic tool P-Elements were engineered

missing the sequence for P transposase, inhibiting their mobility. To cause mutations in the genome circular forms of this nonautonomous P-Elements were injected into the posterior part of embryos, before cell formation. The embryos for this must carry the gene for the transposase and not express the *wt*-inhibitor. For fly transformation the P-Element is replaced by a Plasmid carrying a reporter gene and a gene of interest flanked by the transposase recognition targets **(Rubin & Spradling, 1982; Bier et al., 1989).**

Due to the P-Element' s preference to insert into some specific genes (hotspots) and against insertion into others (coldspots) **(Metaxakis et al., 2005)**, the PiggyBac and the Minos system offer an alternative.

The *lepidopteran* PiggyBac system, is another „Cut & Paste" transposon system used in *Drosophila* genetics **(Thibault et al., 2004)**. The Minos transposon system derived from *Drosophila hydei* of the „Copy & Paste" type is also fully established in *Drosophila melanogaster* as a genetic tool **(Metaxakis et al., 2005)**.

P-Elements are commonly used to create specific Gal4 driver lines. The NP lines for example used in this study are Gal4 enhancer trap lines (P{GawB} element-insertion lines).

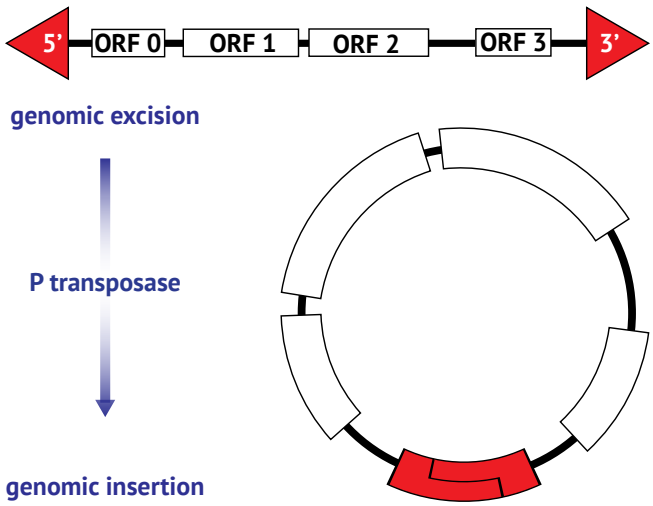

FIG 2.2 | P-Element

The wt P-Element consists of four open reading frames (ORF) which are flanked by 5' and 3' inverse terminal repeats.

These 31 bp long repeats connect when the P-Element is excised from the genome by the transposase.

The motile circular form is reinserted at another position in the genome.

[modified from Ryder & Russel (2003)]

2.1.5 | GAL4 / UAS SYSTEM

The GAL4/UAS system **(Brand & Perrimon, 1993)** facilitates the aimed expression of arbitrary transgenic constructs in certain tissues, cells or at certain stages during development. The system consists of two yeast specific genes, Gal4 and UAS (upstream activating sequence). The gene Gal4 encodes for the transcription factor GAL4. The binding of a GAL4 homodimer to UAS, an enhancer region, starts translation of downstream genes. To use the GAL4/UAS System as a genetic tool in *Drosophila* Gal4 and UAS constructs are randomly or specifically inserted into the *Drosophila* genome by P-Element insertion. If the gene Gal4, under control of a weak promotor, is inserted next to an endogenous enhancer or promotor region, for example a cell specific gene, GAL4 is only expressed in those cells.

Fly lines carrying such constructs are called "driver lines". The "responder lines" carry constructs of a reporter gene X downstream to UAS, which for example can be the gene for GFP. Crosses of transgenic *Drosophila* driver and responder lines are used to investigate problems from genetics to behaviour (see FIG 2.3).

The Gal4/UAS system was used in this study to express Ca^{2+} sensors specifically in *Drosophila* CHOs. For crossings always 3 virgin females and 3 male flies of either the responder or the driver line were used. Different markers of balancer chromosomes were used to identify the desired offspring. Balancer chromosomes do not recombine with homologous chromosomes and mostly carry a mutation with a phenotype easy to identify.

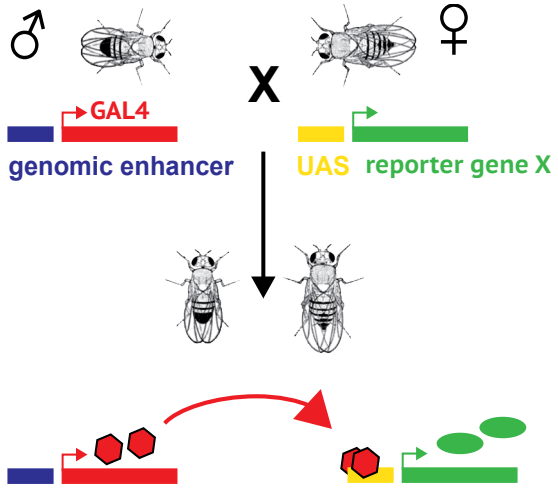

FIG 2.3| Scheme of the Gal4/UAS system

Driver lines expressing GAL4 and responder lines carrying a reporter gene downstream of UAS are crossed to activate a reporter gene in a cell or tissue dependent manner.

In flies of the F1 progeny, the GAL4 homodimer binds to UAS, activating the reporter gene X.

[modified from Brand & Perrimon (1993)]

2.1.6 | Fly Strains

The following *Drosophila melanogaster* fly strains were used for the experiments:

Chart 2.2 | Fly strains

Name	Class	Genotype 1st / 1st ; 2nd / 2nd ; 3rd / 3rd (chromosome)	FlyBase ID vel Donor
EMAP: dsRed2	UAS - marker	*+/+; Sp/Cyo ; UAS-DCX-EMAP:dsRed2 / TM6b*	S. Bechstedt
Cam2.1	UAS - Ca^{2+}sensor	*+/+; UAS-Cameleon2.1 / Cyo ; NP0761-Gal4 / TM6b*	A. Fiala
NP 0761	GAL4	*w- ; Sp/SM1 ; NP0761/TM65bTb*	Nippon Consortium
NP 1046	GAL4	*NP1046-Gal4 / FM7c(Sn+) ; +/+ ; Sb / TM3 Ser*	Nippon Consortium
NP 6250	GAL4	*+/+ ; NP6250-Gal4 / Cy ; MKRS / TM6b*	Nippon Consortium
JO15	GAL4	*w- / w- ; +/+ ; Jo15-Gal4 / TM3-830*	Nippon Consortium
ato^{-}	mutant	*+/+ ; +/+ ; ato[1] / Df(3R)p[13]*	FBgn0010433 FBab0002853
iav^{1}	mutant	*iav^{1} / FM7c(sn+) ; +/+ ; NP0761-Gal4 /TM3 Ser*	FBst0300199
Canton S	wt	+/+ ; +/+ ; +/+	FBst0000001

2.1.7 | Crossing Scheme for Johnston's Organ Experiments

Starter lines

+/+; Sp/cyo ; DCX-EMAP:dsRed2 / TM6b | *+/+; Cameleon2.1 / Cyo ; NP0761 / TM6b* | *iav1 / FM7c(sn+) ; +/+ ; NP0761/TM3 Ser*

Crossing Scheme

iav1 / FM7c(sn+) ; +/+ ; NP0761/TM3 Ser

X

+/+; Cameleon2.1 / Cyo ; NP0761 / TM6b

=

+/FM7c(sn+) ; +/Cy ; NP0761/TM6b X *+/FM7c(sn+) ; +/ Cameleon2.1 ; NP0761/TM6b*

=

+/FM7c(sn+) ; Cameleon2.1 /Cy ; NP0761/TM6b ;

iav1 / FM7c(sn+) ; +/+ ; NP0761/TM3 Ser

X

+/+; Sp/cyo ; DCX-EMAP:dsRed2 / TM6b

=

+/ FM7c(sn+) ; +/Cyo + ; NP0761/ DCX-EMAP:dsRed2 X *+/ FM7c(sn+) ; +/Sp + ; NP0761/ DCX-EMAP:dsRed2*

=

♂ *FM7c(sn+) ; Sp/Cyo + ; NP0761/ DCX-EMAP:dsRed2*

X

♀ *iav1 / FM7c(sn+) ; +/+ ; NP0761/TM3 Ser*

=

iav1/ FM7c(sn+) ; +/Cyo + ; NP0761/ DCX-EMAP:dsRed2 X *iav1/ FM7c(sn+) ; +/Sp + ; NP0761/ DCX-EMAP:dsRed2*

=

♀ *iav1/ FM7c(sn+) ; Sp/Cyo + ; NP0761/ DCX-EMAP:dsRed2*

X

♂ *FM7c(sn+) ; Cameleon2.1 /Cy ; NP0761/TM6b*

=

iav1 / FM7c(sn+) ; Cameleon2.1/ Cyo ; NP0761/ DCX-EMAP:dsRed2

♂ = male ♀ = female virgins

2.2 | Calcium Imaging

2.2.1 | Calcium Imaging Setup

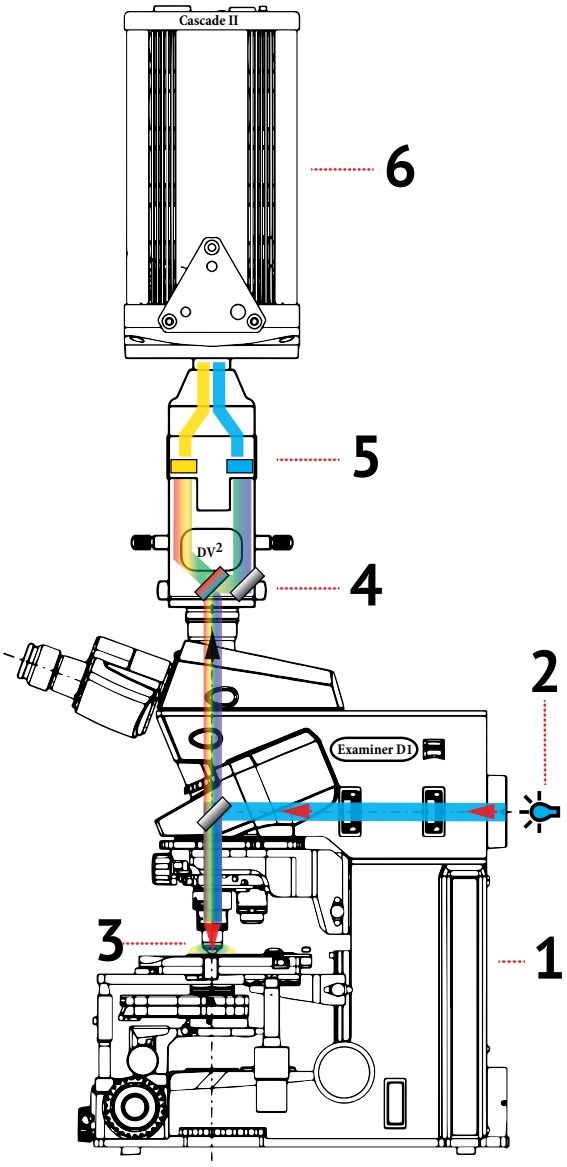

FIG 2.5 | Scheme Ca^{2+} - Imaging-Setup

1| Zeiss Axio Examiner D1 2| Polychromator 3| Objective 4| 515nm DCLP 5| Bandpass Filter 6| CCD Camera [modified from manufacturers manuals]

The setup was built on an actively damped optical table. The Ca^{2+} imaging setup was composed of a microscope, a polychromator, a beam splitter and a CCD camera (see FIG 2.5). Ca^{2+} imaging experiments were realized on a bright field microscope **(Zeiss Axio Examiner D1, Visitron Systems)** (see FIG 2.5| 6) modified for fluorescence microscopy. A prism based polychromator was used for fluorescence illumination, producing user selectable monochromatic wavelengths between 350 nm and 600 nm with an accuracy of ~4 nm **(Visichrome High-Speed Polychromator System, Visitron Systems)**(see FIG 2.5| 2) In all Ca^{2+} imaging experiments the polychromator was tuned to 438 nm, as all specimen used in the experiments expressed Cam2.1 (see 2.1.6). The emitted light of the fluorescent specimen was split by a DiChroic Long Pass filter **(515 nm DCLP)** creating two identical images of different wavelengths **(Dual View 2 imaging system, MAG Biosystems)** (see FIG 2.5| 4). Specific filters **(485/40 nm [CFP] & 535/30 nm [YFP] bandpass filter; 520 - ∞ nm [YFP /dsRED2] long pass filter, Chroma Technology)** narrowed the wavelengths of both image pathways (see FIG 2.5| 5). The aligned images were detected side by side on a single 512 x 512 pixel CCD camera **(Cascade II:512, Photometrics)**.

The average intensity of regions of interest (ROI) for each wavelength channel were recorded online by MetaFluor Software **(Molecular Devices) (Fiala A, 2003)**. The data was post processed in Excel and Matlab (chapter 2.2.5).

2.2.2 | FCO: Leg Preparation and Experimental Procedure

To measure neuronal activity in the chordotonal sensilla of the *Drosophila* FCO I developed a measurement chamber **(Kamikouchi & Wiek et al., 2010)**.

The chamber was made of transparent acrylic glass. A cavity was carved out, which is 3mm in length and 1mm in width and depth. A parallel running cavity, with a quadratic diameter of 0.9 mm, works as a rail for a small acrylic rod connected to a piezo electric actuator **(P-841.10 PZT/Driver, Physik Instrumente)** (see FIG 2.6| 3).

For experiments flies expressing Cam2.1 under control of chordotonal organ specific driver lines NP1046, NP6250, NP0761 & JO15 were used **(Kamikouchi et al., 2006)**. All flies were under CO_2 anaesthesia during preparation. The left wing and all legs, but the right metathoracic leg, were removed from the flies. These flies were quickly transferred to the cavity and fixated with dental UV-glue **(Kentoflow, Kent)**. The femur of the remaining leg was positioned parallel to the rod. The femur-tibia joint was free to move. The tarsae and the distal part of the tibia were glued to the rod. A drop of glycerol was put directly on top of the region that houses the FCO. Then a coverglass was placed over the cavities in a way that only the femur is bathed in the glycerol and the rod with

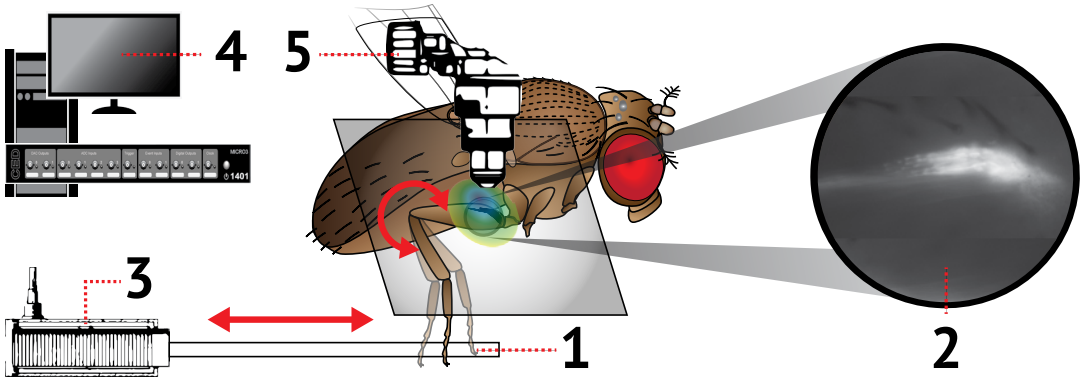

FIG.2.6 | FCO Setup

1| Tibia & Tarsus glued to the acrylic rod; 2| Image of the FCO in MetaFluor; 3| Piezo actuator; 4| PC & A/D converter; 5| Objective; → The red arrows indicate the linear movement of the Piezo actuator and the angular deflection of the tibia towards the femur.

the tibia and tarsus attached was not touching it. The measurement chamber was then placed under the Ca^{2+} imaging setup, in a way that the whole FCO was directly under the objective (see FIG 2.6| 5 & 2). The tibia was deflected by a piezoelectric actuator with step, ramp, staircase and sinusoidal stimuli. The actuator was controlled by Spike2 software via an A/D converter **(micro 1401 MKII, Cambridge Electronic Devises)** (see FIG 2.6| 4). In MetaFluor one ROI was set enveloping the whole organ (see FIG 2.6| 2). For Data processing and analysis see chapter 2.2.5.

2.2.3 | JO: Antennae Preparation and Experimental Procedure

For experiments *iav1* mutant and non mutant *wt*-flies were used. To specifically localize the region of the ciliary dilation, the flies expressed DCX-EMAP:dsRed2, a fusion protein of Emap and the red fluorescent molecule DsRed2 **(Bechstedt et al., 2010)**. DCX-EMAP:dsRed2 localizes to the ciliary dilation. Before preparation, the flies were either chilled on ice for 5min or shortly anaesthetized with CO_2. Then all legs were dissected. A cover slip was prepared with a line of dental glue **(Kentoflow, Kent)**, in the length of the wingspan. Then the dorsal part of the thorax and the wings stretched to the sides were placed on this line. The head was glued to the thorax and the leg stumps were sealed with glue to prevent dehydration. The left antenna was glued to the left eye. To avoid movement of the pedicellus a small amount of glue was put between it and the left antenna. Glycerine was then used to close the gap between the pedicellus, covering the JO. The cover slip was then transferred to an acrylic glass device with two unidirectional micromanipulators, both holding sharpened tungsten electrodes. One electrode, used for grounding and charging the animal, was in the thorax. The other electrode was placed behind the free rotating arista of the right antenna. The acrylic glass device was then placed under the Ca^{2+} imaging setup so that the JO was visible through the objective (see FIG 2.7| 1,3,4,8). Before experiment start the free fluctuations best frequency of the flies antenna was monitored. The displacement of the arista was detected by a laser-doppler-vibrometer (LDV; OFV-534 Polytec) (see FIG 2.7| 1,6 & chapter 2.3). Then a charge of -42 V was applied through the thoracic electrode to the animal (see FIG 2.7| 3). The actuator electrode was connected to a non

commercial amplifier. The arista was then displaced, by changing the voltage of the actuator electrode, alternating back and forth from negative to positive at the fly's best frequency (see FIG 2.7| 4). The stimulus form was set by Spike2 and created by an A/D converter **(micro 1401 MKII, Cambridge Electronic Devises)**. This signal was amplified by the self build amplifier with the factor 1000. As *wt*-flies show the highest antennal nerve response at best frequency stimulation with displacement amplitudes of ~1000nm (see chapter 1.3.2), the displacement was levelled to this amplitude. This was done by de- or in-creasing the actuator electrode and arista inter-distance. After all settings are set the LDV is turned off to prevent crosstalk of the laser beam with the channel set for DCX-EMAP:dsRed2 **(520 - ∞ nm [YFP /dsRED2] long pass filter, Chroma Technology)**. The polychromator was tuned to 557 nm. Pictures of DCX-EMAP:dsRed2 were acquired by MetaFluor. A ROI was set around the region of the ciliary dilations which were marked by DCX-EMAP:dsRed2. Then the excitation wavelength was changed to 438 nm and ROIs were set enveloping the distal part of the cilium, the proximal part of the cilium, the nerve cell bodies and a control region without fluorescence. For data processing and analysis see chapter 2.2.5.

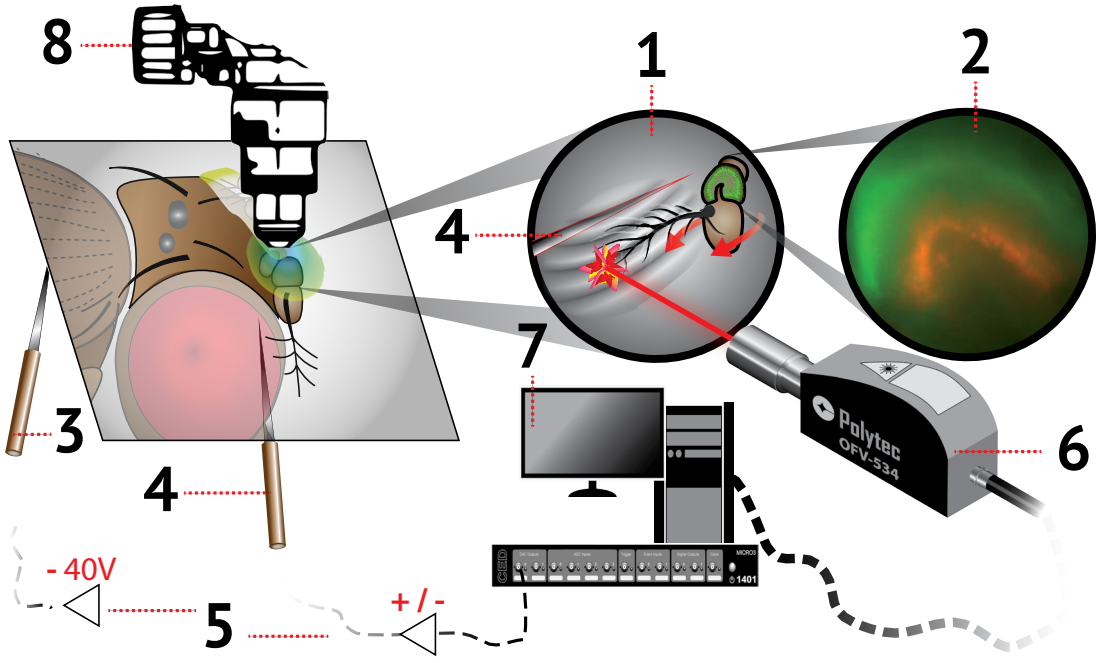

FIG 2.7 | JO Setup

1| Scheme of arista displacement by the actuator electrode 2| Fusion image of the JO (green: Cam2.1, red: Dcx-Emap-Dsred2); 3| loading electrode; 4| actuator electrode; 5|voltage amplifier;
6| LDV: OFV-534 Polytec; 7| PC & A/D converter 8| objective; → The red arrows indicate the movement of the arista and the third segment.

2.2.4 | Data Processing and Analysis

The time traces for fluorescence intensities of eCFP and eYFP were recorded with MetaFluor. The ratio of the two corresponding fluorescent signals of Cam2.1 was calculated as acceptor / donor for every time point. For the FCO experiments, just one ROI was analysed, whereas 5 ROIs were analysed separately for the JO experiments. For FCO experiments data was processed in Excel by a self written macro. First the data was normalized as percental change in fluorescence intensity. This is done by calculating $\Delta I/I_0$ (%) for each stimulus repeat, where I_0 is the baseline before stimulation and ΔI is the change in fluorescence intensity I from baseline I_0.

$$\Delta I/I_0\ (\%) \frac{I(t)-I_0}{I_0}$$

In the FCO experiments I_0 was calculated as the average from a time range before stimulation which was as long as the stimulation itself. As the ratio represents the relative strength of FRET and therefore changes in Ca^{2+} concentration, $\Delta R/R_0$ (%) was calculated like $\Delta I/I_0$ (%). As the recording frequency of the CCD camera had a jitter, all $\Delta I/I_0$ (%) and $\Delta R/R_0$ (%) values were binned to 5Hz. The original frame rate varied from 6 to 10 Hz between experiments. For direct analysis and staircase like stimulation all responses to a certain stimulus repeat were then averaged and plotted over time (see chapter 3.3.2). For further analysis binned data points obtained for baseline corrected Ratio change (ΔR/R0) of repetitions for a certain stimulus were pooled (see chapter 3.3.1).

For JO experiments the data was processed and analysed with Matlab (Version R2010b, Mathworks, Waltham, MA, USA). The baseline was the time range before stimulation, which was as long as the stimulation itself. These data points were fitted with a linear fit. This fit was used to create a time dependent baseline $I_0(t)$.

$$\Delta I/I_0(t)(\%) \frac{I(t)-I_0(t)}{I_0(t)}$$

In the same way $\Delta R/R_0(t)$ (%) was calculated. The use of a time dependent baseline corrected for bleaching. As the recording frequency of the CCD camera had a jitter, all $\Delta I/I_0$ (%) and $\Delta R/R_0$ (%) values were down sampled to a resolution of 5.95Hz. All responses to a certain stimulus repeat were then averaged and plotted over time.

2.3 | Laser Doppler Vibrometer

A Laser Doppler Vibrometer (LDV) allows contactless measurement of an object's surface vibrations. The LDV produces a laser beam which is aimed at a surface of interest. The object's surface vibrations lead to a doppler shift in the reflected laser beam frequency. From this doppler shift the frequency and the amplitude are extracted. This frequency shift can be described as $f_D = 2 * v/\lambda$,

where v is the velocity of the target and λ is the wavelength of the light.

To calculate the velocity of an object the frequency shift has to be measured at a known wavelength. Therefore the LDV uses an interferometer. The interferometer superimposes the intensities of a reference beam I_1 and a measurement beam I_2. This intensity is modulated by the formula:

$$I_{tot} = I_1 + I_1 + 2\sqrt{(I_1 * I_2 \cos * [2\pi * (r1 - r2)/\lambda]}$$

This formula holds an interference term that relates to the path length difference of reference and measurement beam. If this difference is an integer multiple of the laser wavelength, the overall intensity is four times a single intensity. Correspondingly, the overall intensity is zero if the two beams have a path length difference of half of one wavelength **(Basic Principles of Vibrometry; polytec.com)**. The LDV's used can precisely record velocities in the mm/s to nm/s range.

For experiments PSV-400 and OFV-534 were used. The OFV-534 was used for all Calcium Imaging experiments as well as for the locomotion assay and posture control experiments. Changes in free fluctuation and sound induced intensity characteristics of mutant *iav*^{1} flies were measured by PSV-400.

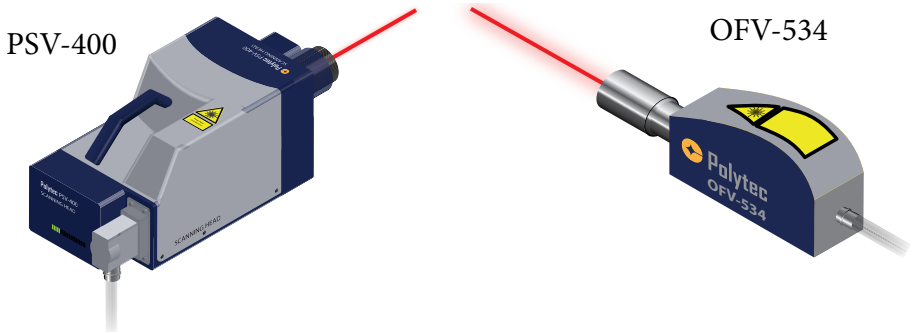

FIG 2.8 | Laser Doppler Vibrometer [Sketch of PSV-400 used on the authority of Dr. Christian Spalthoff]

2.4 | Mechanical Measurements of Sound Receiver Movement

2.4.1 | Setup

CO_2 anaesthetized flies were fixated with hot wax on a Teflon rod. The left antenna was glued to the left eye with UV-glue. To avoid movement of the pedicelus a small amount of glue was put between it and the left antenna. The rod was attached to a micromanipulator and the fly was oriented so that the arista of the right antenna was in the focal point and perpendicular to the LDV (PSV-400) laser beam (see FIG 2.9| 8). A loudspeaker (Visaton W130S) 10 cm behind the fly was used for acoustical stimulation and a microphone was used as reference (see FIG 2.9| 4). The microphone was placed ~ 5mm in distance to the arista and the sound receiving element perpendicular to the loudspeaker. The microphone voltage output was converted to m/s. To record the compound action potential (CAP, [µv]) of the antennal nerve response a tungsten recording electrode was inserted into the head and a ground electrode was placed in the thorax (see FIG 2.7| 3,4). The CAP was amplified (Extracellular amplifier: MA102) and recorded by an A/D converter **(micro 1401 MKII, Cambridge Electronic Devises)** and Spike2 software.

FIG 2.9 | Mechanical Measurement Setup

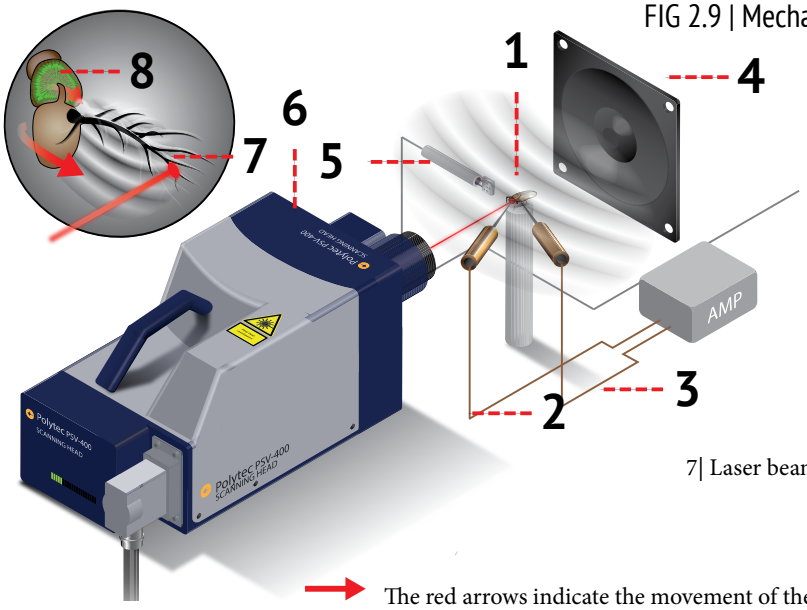

1| Fly fixated on Teflon rod

2| recording electrode

3| ground electrode

4| loudspeaker

5| mircophone

6| LDV(PSV-400

7| Laser beam pointed at rotating arista tip

8| Johnston's Organ

→ The red arrows indicate the movement of the arista and the third segment.

[Modified sketch on the authority of Dr. Christian Spalthoff]

2.4.2 | Free Fluctuation Recordings

The LDV was used to record free fluctuations at the tip of the arista. In absence of stimulation the free fluctuations of the arista were recorded for 100 seconds. Therefore only thermal energy and internal sound receiver processes can contribute to sound receiver movements, recorded as free fluctuations. The LDV software performed online a Fast Fourier Transform (FFT) of the velocity time trace. FFT was calculated as :

$$\dot{X}(\omega)_n = \int_{t_n}^{t_n+1} \dot{X}(t)\, e^{i\omega t} dt$$

This FFT shows the frequency dependent velocity of the arista reflecting the sound receiver specific movement properties. Also the power spectral densities of displacement and velocity were computed by the LDV, for frequencies between 100 and 1500 Hz **(Göpfert & Robert, 2003; Göpfert et al., 2006)**.

To find the best frequency, that means the frequency at which the sound receiver has its maximum deflection amplitude the FFT time trace for velocity can be used or the power spectra were fitted with a simple harmonic oscillator function **(Göpfert et al., 2005)**.

2.4.3 | Antennal Sound Response Characteristics

To asses the specific nerve response of the sound receiver the antenna was stimulated with sound. The stimuli applied were sinusoidal pure tones at the best frequency of the sound receiver. The sound amplitude was modulated over a 90 dB range by an attenuator. 16 different intensities were applied randomly. Stimulus signals were generated via the A/D converter by Spike2 and broadcasted by a loudspeaker.

As described in chapter 2.4.2 the Arista displacement was recorded by the LDV. CAP and microphone output were recorded simultaneously by LDV software and Spike2. Only LDV recordings were used.

The stimulus lasted 1 second and responses to 10 stimulus repeats were averaged. The CAP recordings were normalized to 1 ((V-Vmin)/(Vmax-Vmin)) and plotted against arista displacement and against arista frequency **(Effertz T, Wiek RJ, Göpfert MC, 2011)**.

Both relations were fitted with a Hill-equation to calculate the lower (10% of the Hill-fit) and the upper threshold (90% of the Hill-fit) of the dynamic range **(Senthilan et al., 2012)** .

$$y = y_0 + \frac{ax^b}{c^b + x^b}$$

y0 = minimal y value (> 0),
a = difference of maximum and minimum y value (CAP),
b = sensibility factor (the higher the more sensitive is the system),
c = ymin + ½ (ymax – ymin)

The gain meaning the amplification of the sound receiver in response to a certain stimulus amplitude is calculated as arista displacement over microphone recording. The sensitivity gain was given by dividing the maximum by the minimum gain.

2.5 | Locomotion Assay

2.5.1 | Walking Arena and Experimental Procedure

For studying the effect of substrate vibrations on walking behaviour of *Drosophila melanogaster*, I constructed a walking arena.

The arena was circular and had an inner diameter of 65mm and a height of 2mm (see FIG 2.10| 3). It was made out of white plastic to achieve a maximum contrast towards the flies during recording. To prevent flies from flying away, the arena was covered with translucent acrylic lid. Drilled holes granted air supply. A single LED attached to the lid, was used as visual trigger, emitting 100 ms pulses prior and subsequent to stimulation (see FIG 2.10| 2). Since the spectral sensitivity of all *Drosophila* photoreceptors steeply decrease above 600 nm, a red LED was used (600-700 nm) **(Heisenberg & Wolf , 1984; Harris et al., 1976)** (see also 2.5.2).

A mini shaker, a magnet based machine applied for the dynamic excitation of light objects, was used to move the arena up and down, thus emulating substrate vibrations. A mini shaker (Type 4810, Brüel&Kjær, Nærum, Danmark) was connected by a thread to a screw at the centre of the Arena undersurface (see FIG 2.10| 4). The stimulus pulse duration and amplitude were controlled by Spike2 and applied to the mini shaker by the A/D converter via a specific signal amplifier (Power Amplifier type 2706, Bruel & Kjaer). LED signalling start and stop of stimulation was controlled by Spike2 and the A/D converter. For each trial 15 flies were conveyed from a vial via a mouth pipette

FIG 2.10 | Walking arena

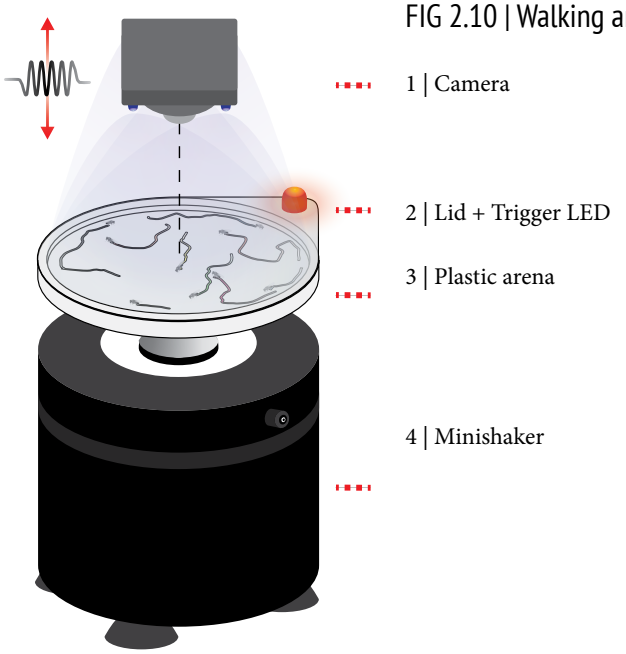

to the arena. Combinations of vibration frequencies (15, 30, 60 & 120 Hz) and vibration amplitudes (1, 5 & 10 µm) were chosen for behavioural experiments. Each stimulus lasted ~500 ms and was repeated 5 times with a 4s interval. Every single fly was only tested once for one specific stimulus setting. Each stimulus combination was tested 5 times. The arena was washed with ethanol and rinsed for every trial.

2.5.2 | Fly Visualization and Tracking

Fly movements were recorded by a digital camera (640 * 480 pixel resolution, Hercules Optical Glass Deluxe) above the arena centre (see FIG 2.10| 1). Since the contrast between flies and background is essential for detecting body axis and orientation, the whole setup was isolated from external light. Four LEDs coupled to the camera illuminated the arena with constant ambient white light. As the photoreceptor adapted to white light the effect of the red trigger lamp can be neglected. The camera frame rate was set to 30 Hz. The recorded trial videos were reviewed in Image J (http://rsbweb.nih.gov/ij/).

This allowed identification of frame numbers for start and end point of stimulus via the red LED flashes. The frame numbers were noticed for further analysis and the video format was changed to RAW. From these videos position and orientation of each fly in every frame were calculated by Ctrax (http://www.dickinson.caltech.edu/ctrax). Ctrax is an automated, quantitative and high – throughput system for analysis of behaviour in freely moving fruit flies **(Branson et al., 2009)**.

The system relies on machine vision techniques enabling automatic tracking of large groups of unmarked flies while simultaneously maintaining their distinct identities. Further processing of the acquired data comprised manual assignments of the exact vibratory stimulation phases, thereby dividing each stimulus trail into three sub periods of equal length (~500 ms), pre – stimulus period, the exact stimulation period and period after stimulation (annotated prestim, peristim, poststim respectively).

2.5.3 | Analysis of *Drosophila* Walking Behaviour

Thrust, slip, yaw, and overall velocities calculated for each video frame were used for analysis. To detect changes in walking velocity the median thrust velocity was calculated for each fly. Flies with walking speeds below 2mm s^{-1} where previously defined as stopping **(Martin et al., 2004; Robie et al., 2010)**. To rule out stopping flies, all flies were neglected with a prestim median thrust velocity below 2mm s^{-1}. Also all fly traces which did not last for the whole experiment were not used for analysis. The medians of all flies for a certain stimulus was calculated and plotted over time. All calculations were performed with Matlab.

2.6 | Posture Control Experiments

To test if *Drosophila* is compensating for substrate vibrations and therefore holds its posture, wild type flies (*Canton S*) and controls were tested. As controls *atonal* mutant flies (*ato*$^{-}$) that lack the FCO (Jarman et al., 1995), were used (see chapter 1.1).

For the experiments the flies were waxed with a soldering iron to a rod. Motion to the sides, front and backwards was limited by insect pins pushed into the wax. Therefore the fly was able to move itself up and down. The rod was attached to a mini shaker (see chapter 2.5.1), displacing it with a sinusoidal stimuli of 3 cycles at a certain frequency and amplitude. Each of this frequency and amplitude combinations was

FIG 2.11 |Posture Control Setup

1 | Mini Shaker

2 | Rod

3 | The fly is fixated at its tarsae to the rod. For better reflection of the LDV laser beam an alloy foil is attached to the thorax.

4 | Laser Doppler Vibrometer centred over the thorax.

5 | Insect Pins preventing side movements

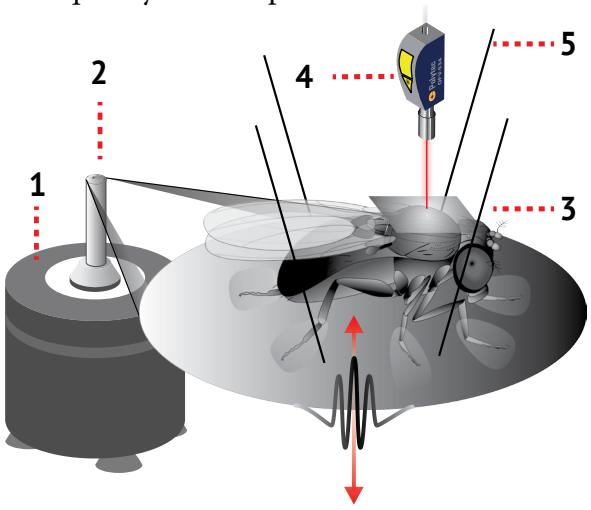

The red arrows indicate the direction of mini shaker movement.

applied ~400 times, for noise compensation. The inter stimulus interval was set to 2 sec.

Before experimental trials the displacement of the rod alone to specific stimuli was recorded by LDV (OFV-534, see 2.3) and Spike2. This recordings were used as reference to displacement of tested flies. For experiments the LDV was placed over the center of the thorax. For better reflection of the LDV beam and to limit effects of the curvature of the thorax a flat piece of alloy foil was glued to the thorax.

Live observation during experiments via a highspeed camera (Casio Exilim EX-FH20) were used to control for impairment of the fixation as well as the integrity of the specimen itself.

The average displacement maxima were calculated online by Spike2 and used for subsequent analysis. The median of the maxima for *ato*$^{-}$ and *Canton S* of different experiments were calculated by MatLab and then compared with the maxima of the stimulus unit. The difference of median maxima towards the stimulus unit were represented as the percentage difference.

3 | Results

3.1 | Ca^{2+} Activity of the Femoral Chordotonal Organ

The effect of different stimuli combinations on the FCO was tested. The FCO response towards these stimuli was monitored as changes in Ca^{2+} concentration via transcuticular Ca^{2+} imaging. Therefore a measurement chamber and a protocol for measurement and data analysis was developed **(Kamikouchi & Wiek et al., 2010; see Chapter 2.2)**.
Different driver lines are known to specifically label subpopulations of the JO **(Kamikouchi et al., 2006)**. These subpopulations were identified by the projection patterns of the labelled JO neurons. Neurons of these subpoluations differ in their response characteristics **(Kamikouchi et al., 2009)** and we found that these functional differences are associated with different activation properties of force-gated ion channels **(Effertz, Wiek & Göpfert, 2011)**.

The driver line NP0761-Gal4 labels all subpopulations of the JO which are: A, B, C, D & E. Subpopulation AB responds to sound and seems to require the NOMPC channel for its mechanosensory function (AB: JO15-Gal4, B: NP1046-Gal4).
Subpopulation CE mediates wind and gravity sensing **(Kamikouchi et al. 2009, Yoruzu et al., 2009)** and seems NOMPC-independent **(Effertz, Wiek & Göpfert, 2011)**(CE: NP6250-Gal4).
These driver lines that label AB and CD neurons in JO are also expressed in the FCO. During my Diploma thesis I could show that NP0761 labels all three subpopulations of the FCO but the expression pattern of the driver lines JO15 and NP1046 do not correspond specifically to any FCO subpopulation **(Wiek, 2008)**.
Ca^{2+} imaging was established using the FCO driver line NP0761, which labels virtually all the FCO neurons and the GECI Cam2.1. Subsequently the other mentioned driver lines were tested. These driver lines (JO15, NP1046 & NP6250) were tested for distinct and/or specific response patterns. No Ca^{2+} responses could be monitored with these driver lines. Thus all Ca^{2+} imaging experiments on the FCO were performed with flies expressing Cam2.1 under the pan FCO driver line NP0761.

3.1.1 | Ca^{2+} Responses Towards Sinusoidal Stimulation

Sinusoids with different frequencies and amplitudes were used to actuate the FCO. The piezoactuator working range limited the maximum peak to peak deflection amplitude to 7.5 µm and and the stimulation frequency to 240 Hz. The intensities of the Cam2.1 FRET pairs eCFP and eYFP and the corresponding ratio change obtained by Metafluor software were postprocessed in Excel (see chapter 2.2.5). Ratio changes (ΔR/R0) were corrected for baseline drifts and pooled for 5 stimulus repetitions.
Pooled responses were fitted with single [f=a*(1-exp(-b*x))] and double exponentials [f = a*(1-exp(-b*x))+c*(1-exp(-d*x))] (see FIG 3.1). Both functions did fit the data. Akaikes information criterion (AIC) **(Akaike, 1973)**, a measure of the goodness of fit was used to select the best model. AIC showed that a single exponential suffices to fit the data. Maxima and time constants of the single exponential were used for further analysis.

To characterize the response characteristics towards sinusoidal stimulation the tibia was deflected at 6 µm peak to peak amplitude and sinusoidal frequencies of 1, 15, 30, 60, 120, 240 Hz. Each frequency was applied five times for 5 sec with a 20 sec repetition interval. Ca^{2+} responses could be monitored for all stimulus frequencies except for 1 Hz since baseline noise was as high as response (see FIG 3.2 | a+b left). The maxima for different frequencies at 6 µm peak to peak amplitude show that higher frequencies lead to a higher calcium response (see FIG 3.2 |b left). Time constants and standard deviation decrease at increasing frequencies (see FIG 3.2 |a left), but all data are in the range of standard deviation. To find a threshold for sensibility of the FCO the tibia was deflected with different peak to peak amplitudes (0.219, 0.4375, 0.875, 1.75, 3.5, 7 & 14 µm) at a certain frequency. Sinusoidal stimulation at 60 Hz was chosen due to the fact that at lower frequencies the detection of calcium signals was often camouflaged by baseline noise and that at higher frequencies the calcium signal seems to saturate. Data was acquired and analysed in the same manner as described for varying frequencies. The maxima of single exponential fit show that peak to peak amplitudes even in the submicrometer range can evoke calcium signals (see FIG 3.2 |a right) and that higher stimulus amplitudes lead to higher Ca^{2+} response. The time

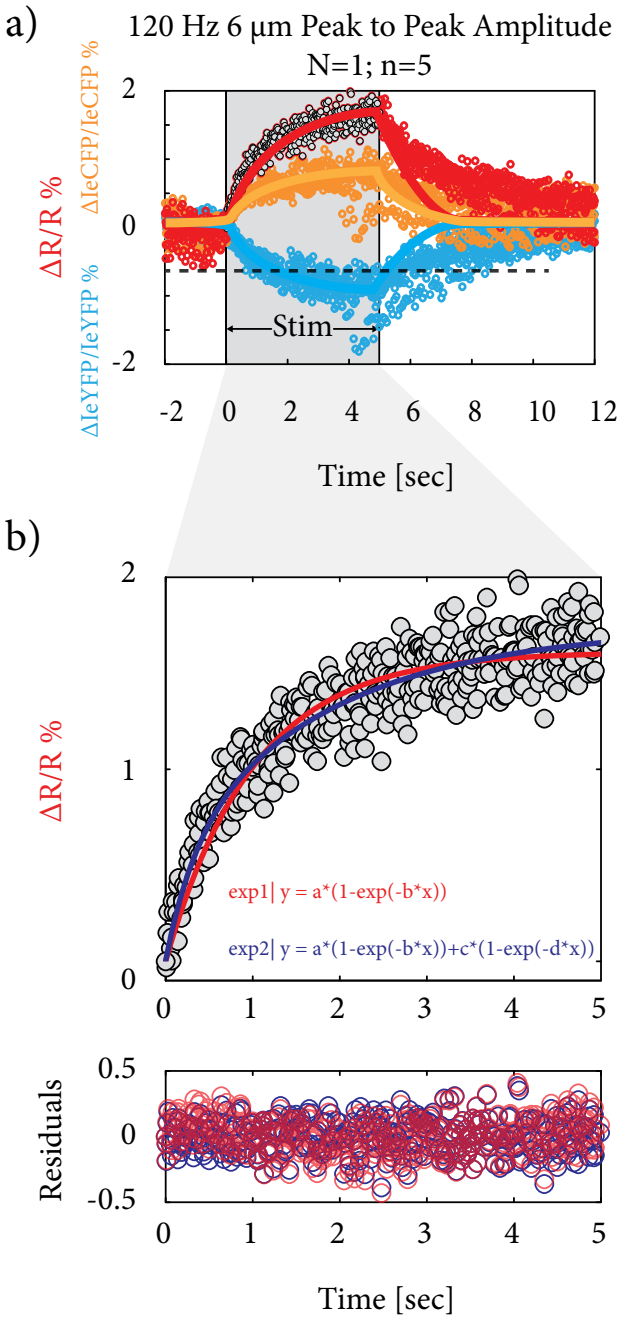

FIG 3.1 | FCO Ca^{2+} Responses to Sinusoidal Stimulation

The tibia was deflected with sinusoidal stimuli of varying frequency and amplitude combinations.
a) FCO Ca^{2+} response of five stimuli repeats pooled. (5 sec 120 Hz sine stimulation 6 µm peak to peak amplitude).
b) The pooled data were fitted by a single and a double exponential. The residuals are evenly distributed for single and double exponential, but AIC shows that the single exponential does fit the data best.
Akaike Information criterion:
AICR2=n ln (1-R2/n)+2k
R2=compares the explained variance (variance of the model's predictions) with the total variance (of the data).
(R2=SSreg/Sstot) SSreg=Σ(fi-y)2, SStot=Σ(yi-y)2; n=number of data points; k=parameters

constants are in the range of standard deviation for all amplitudes applied and therefore not trend for changes in response onset can be observed (see FIG 3.2 |b right).

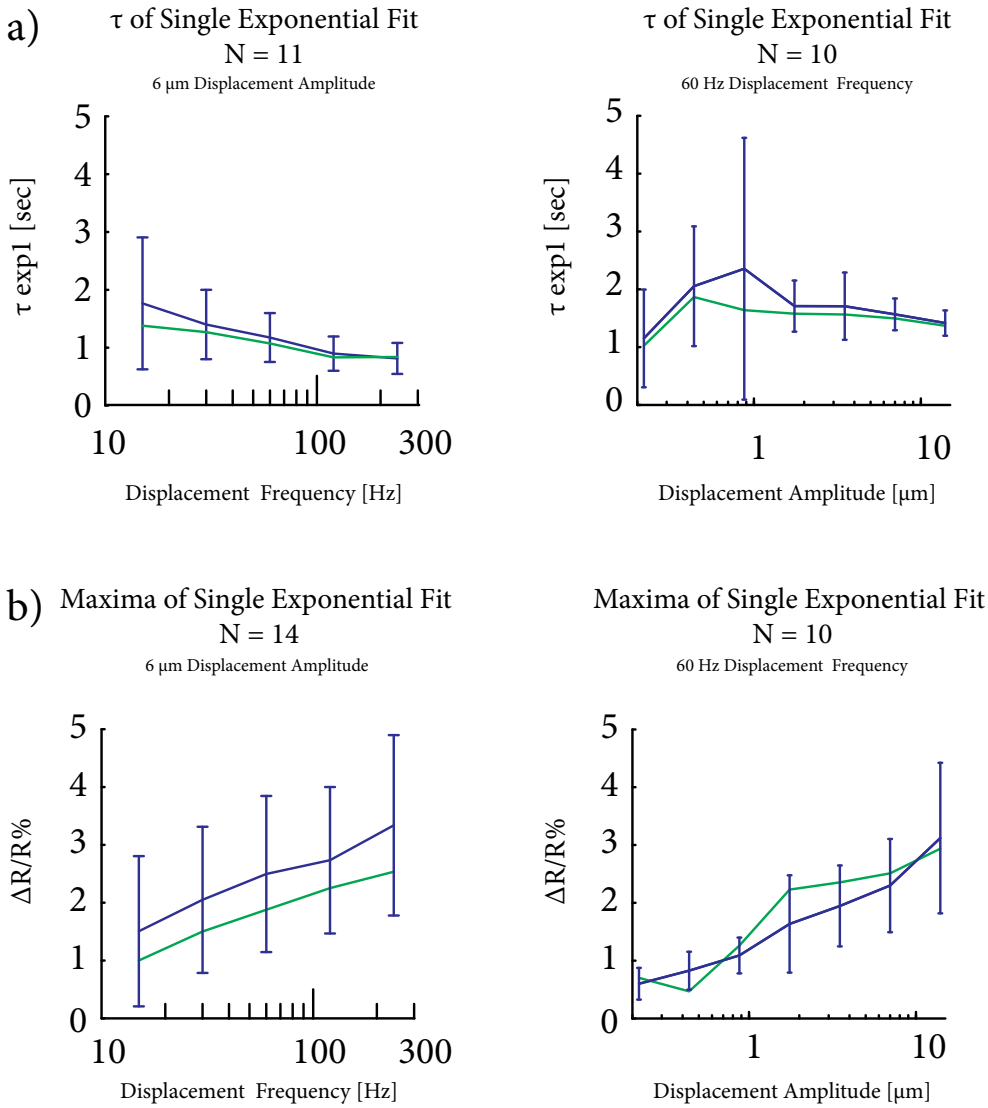

FIG 3.2 | Single Exponential Fit Values of FCO Ca^{2+} Response
a) Mean time constants for frequency (left) and amplitude (right) series.
b) Mean maxima values for frequency (left) and amplitude (right) series.
blue: mean + standard deviation; green: median
Left: The tibia was deflected at 1, 15, 30, 60, 120 & 240 Hz at 6µm stimulus amplitude.
Right: The tibia was deflected at 60 Hz with stimulus amplitudes of 0.219, 0.4375, 0.875, 1.75, 3.5, 7 & 14 µm.
All stimuli were applied 5 times. N = number of specimen

3.1.2 | Ca^{2+} Responses Towards Staircase Like Stimulation

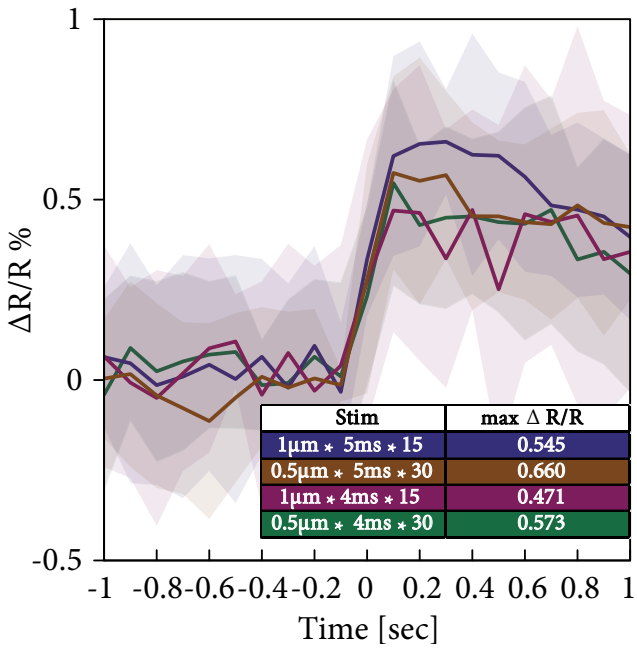

FIG 3.3 | Staircase Like Stimulation of the FCO
FCO Ca^{2+} responses of ten stimuli repeats binned (Binwidth 0.2 sec). (0.5µm * 4ms * 30steps; 1µm * 4ms * 15steps; 0.5µm * 5ms * 30steps; 1µm * 5ms * 15steps) All stimuli applied had an overall amplitude of 15µm. Staircase stimuli at different step amplitudes and interstep length elicit Ca^{2+} responses in the FCO. All stimuli applied had an overall amplitude of 15µm.

To disentangle the effect of position, velocity and acceleration single step and ramp stimuli were applied. No settings allowed by the limitations of the piezoactuator used evoked any measurable Ca^{2+} responses in the FCO.

As single steps and single ramps did not elicit any calcium response, combinations of both were applied. These staircase like stimulation only evoked relative small calcium reponses when interstep length was in the time range of action potentials (FIG 3.3). The limiting factor was the maximum deflection amplitude of the piezoactuator (<15 µm).

3.2 | *Drosophila* Walking Behaviour Towards Substrate Vibrations

To test the effect of substrate vibrations on *Drosophila* walking behaviour, a locomotion assay was developed (see chapter 2.5). The involvement of the FCO in sensing substrate vibration should be investigated by the use of wild type flies and flies missing the FCO. First *Canton S* wild type flies were tested to see if substrate vibrations have any effect on walking behaviour, but a clear response pattern could not be detected. At 15 and 30 Hz, with any amplitude, no change in walking behaviour could be observed. At 60 Hz and at all stimulus amplitudes the median velocity decreases after stimulus onset. For

1 µm and 10 µm stimulus amplitude the walking velocity remains decreased during the peristimulus and the poststimulus period. For 5 µm stimulus amplitude the flies increase their velocity to the prestimulus velocity during the peristimulus period and keep this velocity during poststimulus period. At 120 Hz flies decrease their walking velocity only slightly after stimulus onset. Flies stimulated with 5 and 10 µm stimulus amplitude increase their walking velocity to higher speeds as prestimulus walking velocity. Flies stimulated with 1µm at 120 Hz only slightly increase their walking velocity after peristimulus period. All sub phases are not significantly different by their confidence intervals. These findings show an incoherency in *Drosophila* walking behaviour towards substrate vibrations.

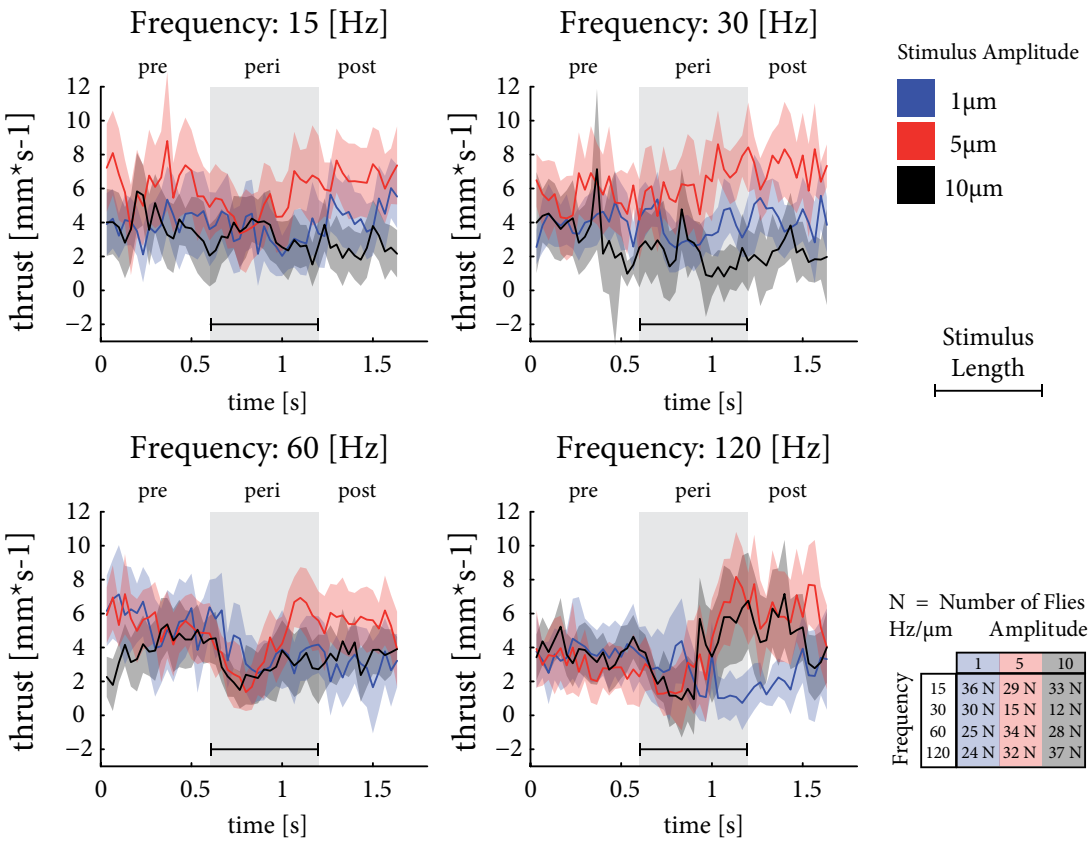

FIG 3.4 | Substrate vibration effect *Drosophila* walking behaviour

Median thrust velocities and confidence interval of walking flies at pre-, peri- & post- stimulus periods for different stimulus amplitudes (1, 5 & 10µm) and frequencies (15, 30, 60, 120 Hz). The stimulus lasted ~ 500ms and was repeated 5 times for each experiment. Flies not tracked by Ctrax for the whole experiment and flies not walking were not analysed (see chapter 2.5.3). No trend can be observed at frequencies 15 & 30 Hz. After stimulus onset at 60 Hz stimulus frequency the flies thrust speed seems to decrease down to the walking threshold of 2mm s^{-1} (see chapter 2.5.3). After a short stop phase flies seemed to start walking again during peristimulus period. At 120 Hz these effects can be only monitored for 5 and 10µm stimulus amplitude, but not for 1µm stimulus amplitude.

3.3 | *Drosophila* Compensates for Substrate Vibrations

To assess if the FCO is required for control of body posture during substrate vibration like displacements, the thoracic displacement of *Canton S* and *ato*⁻ to vertical movements, emulating substrate vibrations, were recorded (see chapter 2.6). Stimuli combinations of different peak to peak amplitudes (1 µm, 10 µm, 50 µm, 100 µm, 500 µm) and frequencies (15 Hz, 30 Hz, 60 Hz, 120 Hz) were tested. The single experiment average maximum displacement (see FIG 3.5) was used for analysis. FIG 3.5 exemplifies a single experiment for sine displacements, at 60 Hz and 1 mm amplitude, of a *Canton S* wild type fly and an *ato*⁻ mutant fly. The maximum displacement of the *ato*⁻ mutant and the stimulus unit is in the range of standard deviation. The *Canton S* maxima are smaller then the maxima of the *ato*⁻ mutant fly and the stimulus unit. The standard deviations of *Canton S* and *ato*⁻ mutants do not overlap at the maximum displacement. The time difference between the stimulus and the specimen maximum is smaller than 1 msec.

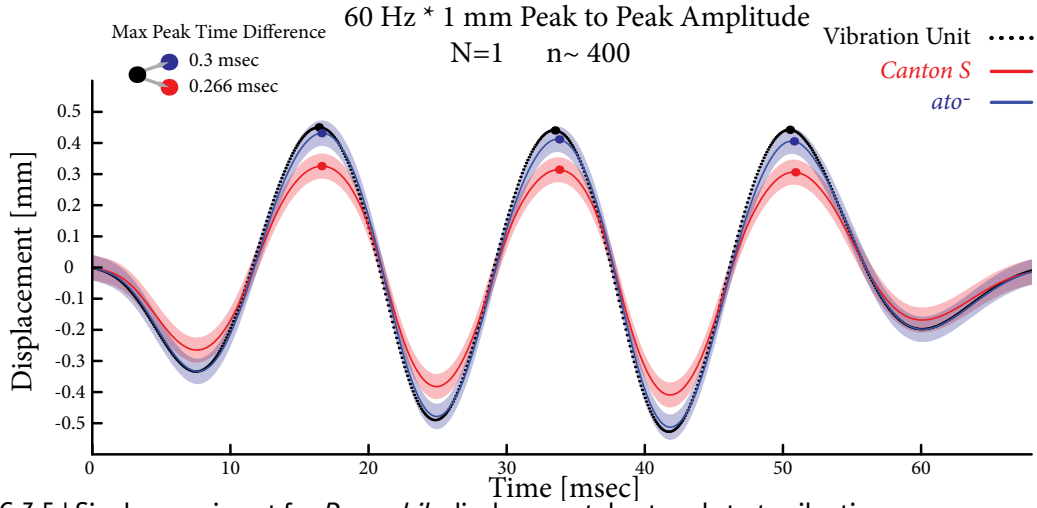

FIG 3.5 | Single experiment for *Drosophila* displacement due to substrate vibrations

Displacement average of the stimulus unit, for an *ato*⁻ mutant fly and a *wt* fly plotted over time. The stimulus, consisting of three sine cycles at 60 Hz and 1mm peak to peak vertical displacement, was repeated with an inter stimulus interval of 2 sec. The coloured dots on the averages tag the positive maximum displacements. N= number of specimen; n= number of stimulus repeats

For further analysis the median of the average maximum displacements was calculated. The percentage difference between the stimulus displacement and the thoracic displacement of the specimen reflects the differences between *Canton S* and *ato*⁻ flies

(FIG 3.6 & 3.7). At deflection amplitudes of 1 µm the thoracic displacement of *Canton S* and *ato-* flies is higher than the displacement of the stimulus unit (see Fig. 3.6, 15 Hz). At these small amplitudes the flies move themselves up and down independent of the stimulus, as shown by live observation (see chapter 2.6). At 10 µm displacement, the thoracic displacement of *Canton S* and *ato*$^{-}$ converge to the stimulus units displacement (see Fig. 3.6 & 3.7|a+b)).

Starting at these displacement values it could be observed that at higher amplitudes the thoracic displacements of the specimen is smaller than the stimulus displacement (see Fig. 3.6 & 3.7). Interestingly the thoracic displacement of *Canton S* is smaller than the displacement of *ato*$^{-}$ flies (see Fig. 3.7| c)). This applies for all frequencies and for all amplitudes higher than 50 µm, except for stimulation at 120 Hz & 50 µm amplitude (see Fig. 3.6 & 3.7). The displacements for *Canton S* and *ato*$^{-}$ are significantly different for all stimulus amplitudes at 60 Hz stimulation (see Fig. 3.7| c+d)).

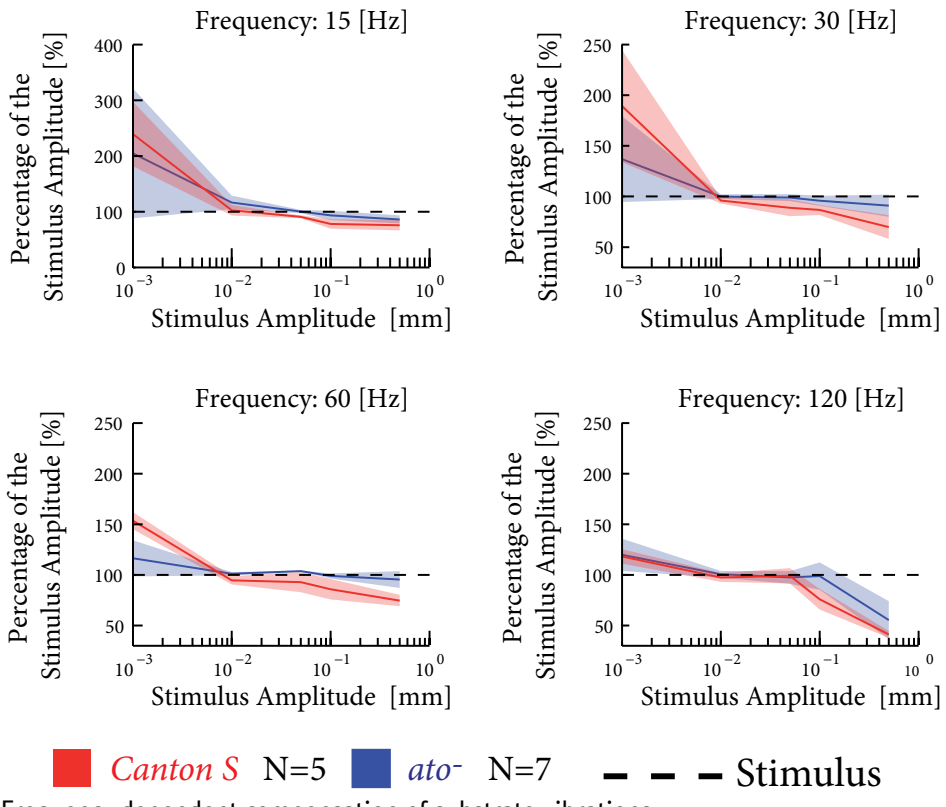

FIG 3.6| Frequency dependent compensation of substrate vibrations

Percentage of the stimulus amplitude plotted over stimulus amplitudes for different stimulus frequencies. The dashed line indicates the stimulus units displacement. The straight lines represent the median displacement amplitudes of *Canton S* (red) and *ato*$^{-}$ (blue). The colour corresponding transparent areas notify the 95% confidence interval. N= number of specimen; n= number of stimulus repeats

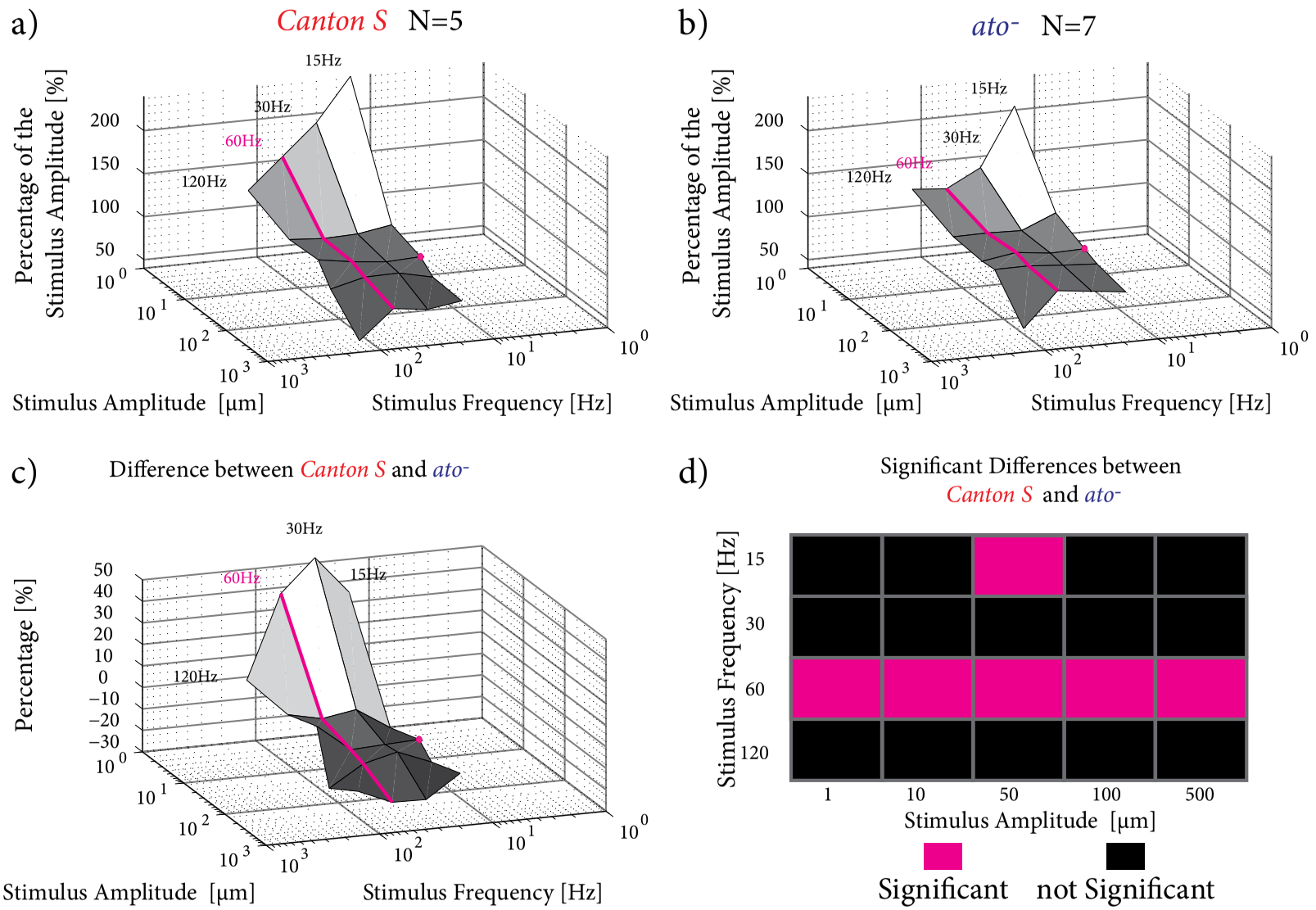

FIG 3.8| Displacement differences between *Canton S* and *ato-*

a+b) Percentage of the stimulus amplitude plotted over stimulus amplitudes and stimulus frequencies for *Canton S* (a) and *ato*⁻ (b).

c) Percentage difference between *Canton S* and *ato*⁻ displacement plotted over stimulus amplitudes and stimulus frequencies. Positive percentages indicate

d) Significant differences between *Canton S* and *ato*⁻ by 95 % confidence intervals of the median. Magenta: significantly different; Black: no significant difference

a-c) The magenta lines indicate significant difference.

3.4 | Ca^{2+} Imaging of JO Neurons in *iav1* Mutant Flies

As mentioned in the introduction the role of TRPN & TRPV channels in *Drosophila* auditory transduction is controversial: Whether NOMPC or NAN/IAV is the primary transduction channel or a direct part of the transduction machinery remains unclear. Missing nerve potentials and altered hyperamplifictaion of *iav* and *nan* mutant flies indicate that transduction is modulated by NOMPC and mediated by NAN/IAV. To unveil if *iav* mutants generate ciliary transduction currents, Ca^{2+} imaging was used.

To image calcium signals in JO neurons in the *iav*[1] mutant background , the following line was generated: *iav[1]/FM7c;Cam2.1,Cam2.1;NP0761/DCX-EMAP:dsRed2* (see chapter 1.3.7 & 2.2.3; chart 2.2). Here, DCX-EMAP:dsRed2, which labels the ciliary dilation **(Bechstedt et al., 2010)**, is used as a landmark.

Male *iav[1]/- or* homozygous female *iav[1]* flies (mutants) and heterozygous *iav[1]/FM7c* (controls) were analysed, and their antennal mechanics were measured prior to the imaging of calcium signals (see FIG.3.7).

The antennal best frequency was ca. 200 Hz for *iav[1]/FM7c* controls and ca. 100 Hz for the *iav[1]* (Figure 3.7| a) **(Göpfert et al., 2006; Lu et al., 2009)**. The power spectral density for *iav[1]* flies is also ~ 150 times higher than in wildtype and *iav1/FM7c* flies (Figure 3.7| a) **(Göpfert et al., 2006)**. The nerve responses of *iav1/FM7c* and *iav[1]* flies also resemble the reported responses for wildtype and *iav* mutant flies. The *iav1/FM7c* flies respond to antennal displacements in the nm range and have a maximum nerve response at around 1000 nm and at even higher displacements show decreased response (Figure 3.7| b) **(Effertz, Wiek & Göpfert, 2011)**. In the *iav[1]* mutants for contrast, no sound evoked nerve response towards antennal displacements were detected (Figure 3.7| b). Recordings of the antennal displacement of *iav[1]* flies also resemble the known characteristic features of increased nonlinear amplification of *iav* mutant flies (Figure 3.7| c) **(Göpfert et al., 2006; Lu et al., 2009)**.

Since the antennal response characteristics of the generated fly strain for *iav1/FM7c* & *iav[1]* flies concur with the characteristics described for wildtype flies and *iav* mutant flies, respectively, the generated fly strains (chapter 1.3.7) were used for the Ca^{2+} imaging experiments. Confocal imaging showed that the Ca^{2+} sensor Cam2.1 was

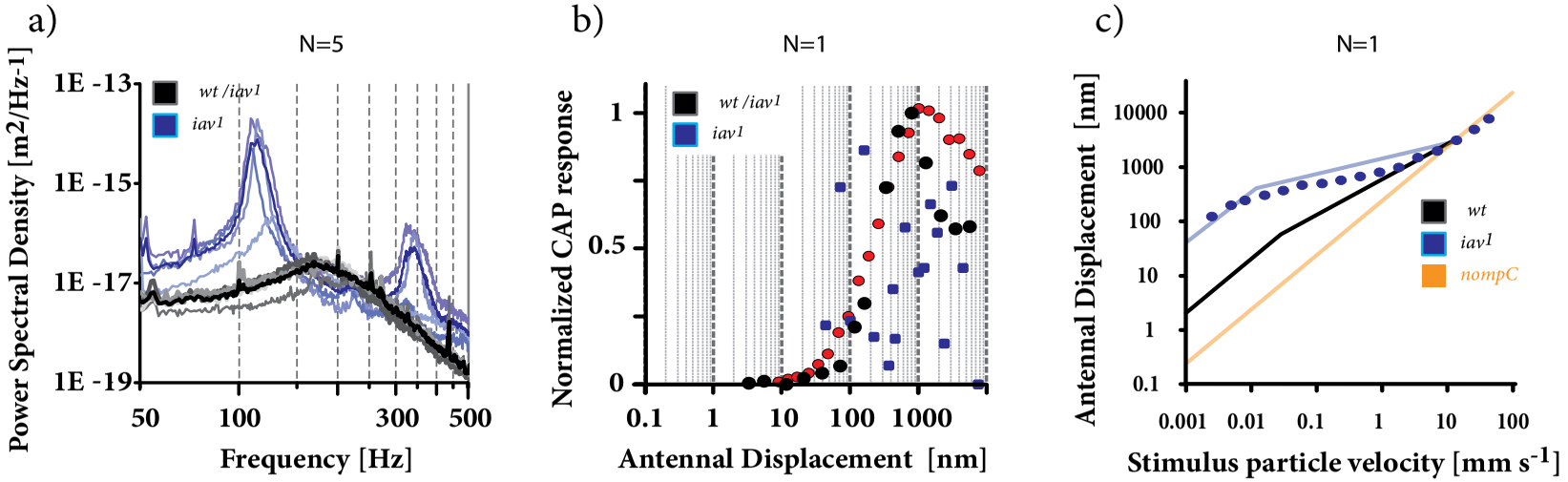

FIG 3.7 | Antennal Response Characteristics of Flies expressing the Ca^{2+} sensor and the Ciliary Dilation Marker

a) Free fluctuations: Power spectra of the sound receiver's vibrations at Brownian motion (No stimulus applied). Blue traces: spectra of 5 *iav*^{1} mutant flies; Grey traces: *wt/iav* flies.

b) Nerve response: Normalized compound action potential plotted against log scaled antennal displacement. The stimulus was played at the antenna best frequency. Blue dots: spectra of 5 *iav*^{1} mutant flies; Grey dots: *wt/iav* flies; Red dots: *wt* flies

c) Nonlinear amplification: Log-log coordinates of the displacement of the fly's antennal sound receiver as a function of the stimulus particle velocity. Displacements and particle velocities are given as Fourier amplitudes at the stimulus frequency, which was adjusted to the individual best frequency of each receiver. The straight lines, resembling nonlinear amplification of wildtype flies, NOMPC & IAV mutant flies are taken over from FIG.1.5.

(here: *iav*^{1} = *iav*^{1}/*iav*^{1};*Cam2.1,Cam2.1; NP0761/DCX-EMAP:dsRed2*; *wt/iav* = *iav*^{1}/*FM7c;Cam2.1,Cam2.1;NP0761/DCX-EMAP:dsRed2*; *wt* = *Canton S*)

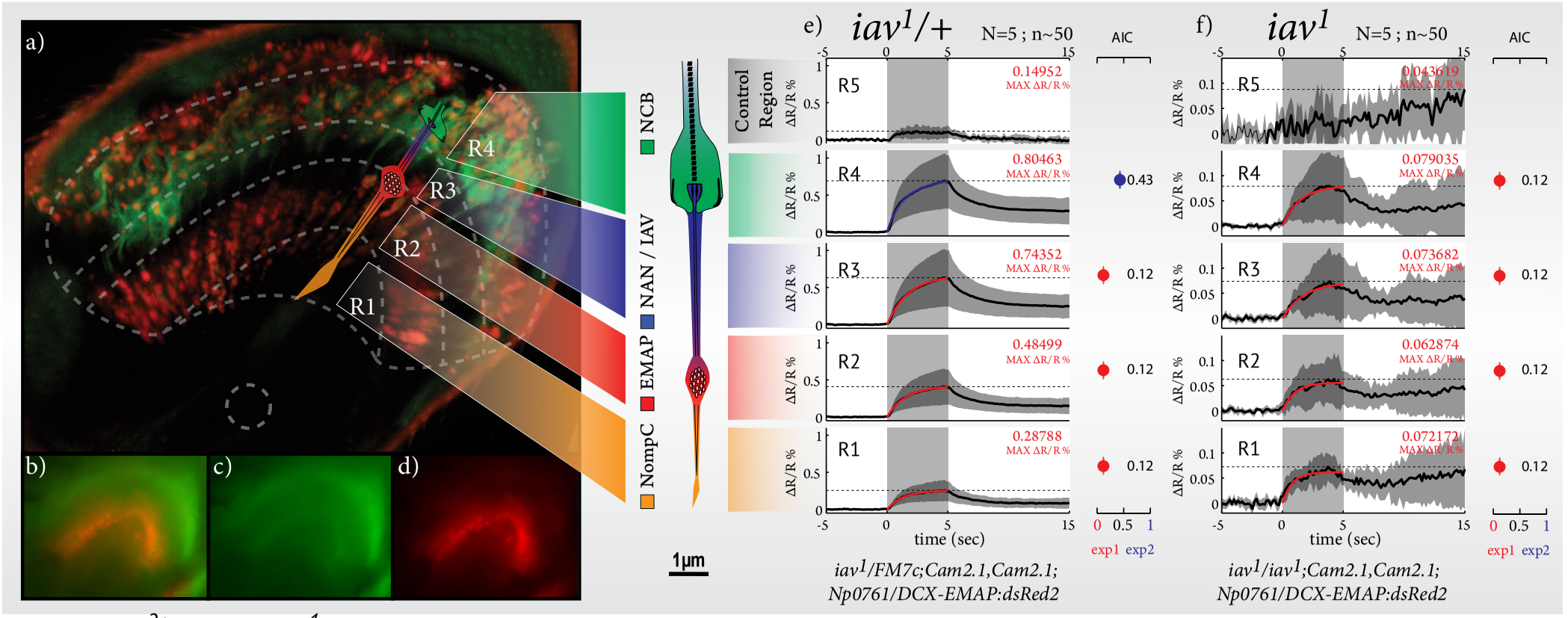

FIG 3.7 | Ciliary Ca^{2+} responses in *iav*^{1} mutant flies

a-d) Images taken from a fly with genotype *iav*^{1}*/FM7c;Cam2.1,Cam2.1;NP0761/DCX-EMAP:dsRed2*; a) Confocal image (True Confocal Scanner Leica TCS SP2, 60x magnification); b) Ca^{2+} imaging setup overlay of channels c+d; c) Cam2.1; d) DCX-EMAP:dsRed2; R1-R5| The ROIs set for Ca^{2+} imaging envelopes specific regions of the Jo's scolopidia; R1| Region of NOMPC localization; R2| Region of DCX-EMAP and ciliary dilation; R3| Region of NAN/IAV localisation; R4| Region of proximal part of the cilium and nerve cell bodies; R5| control Region set outside the JO; e-f) Average Ca^{2+} responses (black lines) & standard deviations (grey background), shown as ΔR/R% over time, towards best frequency stimulation at 1000 nm. The Stimulus was repeated ~50 times. The red lines indicate single exponential and the blue line a double exponential. The dotted grey lines show the average maximum ΔR/R% response, and total numbers are given in red. Right to figures e) and f) the AIC weights are given for the probability that the data are better approximated by a single (0) or a double exponential (1). e) Control: *iav*^{1}*/FM7c* f)Mutant: *iav*^{1} / *iav*^{1}

expressed in JO neurons and that DCX-EMAP:dsRed2 located to the ciliary dilation (see FIG. 3.7| a)). Before Ca^{2+} imaging experiments were performed a ROI (R2) was set around the region of DCX-EMAP:dsRed2, to distinguish between the most distal part and the proximal part of the JO dendrites (see FIG. 3.7| d)). Then ROIs were set around the regions of NOMPC (R1), NAN/IAV (R3) location and around the NCBs (R4) (see FIG. 3.7| a),c)). A control region (R5) was set where no fluorescence could be observed. Subsequently the flie's antenna were stimulated at their best frequency (~100 Hz for *iav*^{1} and ~200 Hz for *iav1/FM7c* ; see chapter 2.2.3) with displacement amplitudes of 1000 nm, which corresponds to the maximum amplitude of the nerve response in wildtype flies. (see FIG.2.6).

The stimulus was applied for 5 seconds and repeated ~ 50 times. Average Ca^{2+} responses, given as ΔR/R%, were recorded from *iav*^{1} mutants and *iav*^{1}*/FM7c* controls. The maximum response increases for *iav*^{1}*/FM7c* from R1 to R4. In the control region R5 of *iav1/FM7c* flies a signal was detected, which is about two times smaller then the response in R1 (see FIG 3.7 | e). In *iav*^{1} flies the signal does not increase from region R1 to R4 (see FIG 3.7 | f). In the control region R5 only noise is detected. The maximum response in *iav*^{1} mutants is around 0.07 ΔR/R% for all regions (see FIG 3.7 | f). This value is around 4 times smaller than the maximum response in region R1 and around 11 times smaller than the maximum response in region R4 of *iav1/FM7c* flies.

Single and double exponentials approximate the average Ca^{2+} response of *iav1/FM7c* and i*av*^{1} obtained from all regions (see FIG 3.7 | e) & f); see chapter 3.1). AIC weights provide a measure of the probability that one model serves as a more sufficient approximation to the data than the other. AIC weights can assume figures between 0 and 1, whereas in this case 0 is low probability and 1 is high probability that the double exponential fits the data better than the single exponential. AIC weights are equal for all regions in *iav*^{1} flies and for regions R1 to R3 in *iav1/FM7c* flies, with an AIC weight of 0.12. Only in region R4 *iav1/FM7c* flies the AIC weight is higher with a value of 0.43. By this, one can assume that a secondary process alters Ca^{2+} response in -or proximally of- region R3, to which Iav localizes.

4 | Discussion

According to the results, the femoral chordotonal organ selectively responds to vibratory stimuli and is necessary for control of body posture during substrate vibrations. Next to this the results indicate a slight effect of substrate vibrations on walking behaviour. The results also show that JO neurons still display sound-evoked calcium signals in the absence of TRPVs.

4.1| Functional Properties of the *Drosophila* FCO

4.1.1 | The FCO Detects Frequency Dependent Stimuli

The observation that the FCO responses to sinusoidal stimulation at amplitudes down to about 100 nm is highly remarkable. This leads to the assumption that the FCO or part of the FCO's scolopida, might be a detector for substrate vibrations.
The stair case like stimulations support this, as the frequency with which the steps were ramped was 200 to 250 Hz. This corresponds to the frequencies of the sinusoidal stimuli applied. It has been reported that substrate vibrations provide information used in different behavioural aspects such as courtship, predator prey interactions, recruitment of food and **(Hill, 2001; Fabre et al., 2012)**. Therefore an behavioural assay investigating *Drosophila's* response to different substrate vibrations was established during this thesis.
The results presented here indicate that the femoral chordotonal organ neither responds to step nor ramp actuation. Two possible explanations exist:

First changes in calcium concentration could be so small that the change in FRET ration is masked by the baseline noise of the calcium sensor Cam2.1. Also it could be that only certain neurons respond to step or ramp stimuli and that their response is overlaid by the baseline fluorescence, as all FCO neurons express Cam2.1.

Second, the FCO does not respond to steps and ramps, or the deflection amplitude is too small to account for a sufficient response. This Theory seems feasible regarding the size of the *Drosophila* leg and the way it is moved by the piezoactuator. The tibia is about 400 µm in length which is deflected between 0.219 µm and 14 µm which leads to angular changes at the femorotibial joint of 0.03° and 2°. It was shown in a previous study that the stick insect's FCO responds to ramp stimuli with 10°- 60° angular changes of the femorotibial joint **(DiCaprio et al., 2002)**. The limitation in stimulus amplitude in the experiments described here may explain the inability to detect Ca^{2+} changes of step or ramp stimuli. Also the changes in calcium concentration can be masked by the baseline noise of the calcium sensor Cameleon2.1. To overcome this obstacle a wider range in angular deflection of the tibia or a mathematical approach to reduce signal to noise ratio would be needed.

4.1.2 | Substrate Vibrations Slightly Affect *Drosophila* Walking Behaviour

The effect of substrate vibrations on Drosophila walking behaviour can were observed at 60 and 120 Hz At 60 Hz, the flies transiently decreased their walking velocity upon stimulus onset but speed up again at midst of the stimulus. The primary response and the following acceleration could indicate a reflex based startle response. For 120 Hz a similar trend was observed, but the videos revealed that some flies lost contact to the ground and were spun around. The assumption that substrate vibrations have an effect on *Drosophila* walking behaviour could not be finally confirmed. Responses indicating either fright or flight behaviour, meaning stopping or an increase in walking velocity could not be identified. There are no significant differences in walking behaviour between the defined stimulus sub phases (prestim, peristim, poststim) even for stimulation at 60 Hz. Possible explanations for these findings include:

First it is obvious that the mean velocity recorded at the prestim phase is with ca 6 mm/sec around 3 times smaller than the values observed by Branson et al. and Robie et al for walking flies. **(Branson et al., 2009; Robie et al. 2010)**. This reduced walking velocity could result from the fact that a lid was used to prevent escape by flight. Branson et al instead performed their experiments with wing clipped flies in an open arena. The

relative small space between the thorax and the lid possibly disrupted normal walking behaviour, as flies could touch the lid with their thoracic bristles. As it is known that *Drosophila*, if given a choice approaches the closest object **(Robie et al. 2010)**, the arena design itself could distract normal walking behaviour. Branson et al used a heat barrier to prevent flies from walking at the arena edges **(Branson et al., 2009)**.

Secondly the stimulus itself could be in adequate to elicit a behavioural response, as it simulates substrate vibrations as a pure vertical displacement on all legs at the same moment.

It is known for insects that they detect substrate vibrations as traveling waves **(Bell, 1980)**. Recently discovered abdominal substrate tremulations causing stopping in females during courtship, show that substrate vibrations have an effect on Drosophila walking behaviour **(Fabre et al., 2012)**. The fact that these substrate vibrations are transmitted via the legs **(Fabre et al., 2012)** provide further evidence that the FCO could be a detector for substrate vibrations. The relative small amplitudes of around 200 nm **(deduced from velocity traces in Fabre et al., 2012)** at around 200 Hz for the abdominally created substrate vibrations are in the Ca^{2+} response range of the FCO. Adjustments of the experimental setup and the stimuli, as well as observing flies during courtship and the use of flies which lack the FCO could clear if Drosophila detects substrate vibrations via the FCO. If a significant response can be detected with these adjustments, it could also help to distinguish if the response is PNS or CNS based. The presence of peripheral synapses emanating from the FCO in form of the glomerulus point out to reflex based effects of the FCO. It has to be identified if the glomerulus has efferent inputs from moto-neurons or afferently contacts these. The technique of GFP reconstitution across synaptic partners (GRASP) **(Feinberg et al., 2008)**, by expressing split GFPs from sensory and motoneuronal side, could answer this question.

4.1.3 | The FCO is Necessary for Posture Control

Drosophila does compensate for substrate vibrations by control of its body posture.

Drosophila controls its body posture by pulling its legs to the body to compensate for upward displacement and accordingly stretching its legs away when displaced

downwards. This leads to a relative stable body position during displacement. The significant differences of thoracic displacement of wildtype flies and *atonal* mutants that lack the FCO, at 60 Hz stimulation, shows that the FCO is necessary for the control of body posture during substrate vibrations. The time differences between stimulus vibration and the body vibration of 0.26 msec for wildtype and 0.3 msec for *atonal* mutant flies are, which leaves no time for synaptic transmission. This means it is a passive feature, probably resulting from the recording of a non even surface, which are the specimen compared to the even surface of the stimulus unit. The fact that there is no phase shift with a longer duration between the stimulus unit and the specimen, raises the question how the FCO controls compensation for substrate vibrations. The previously mentioned influence of the glomerulus is also to long for direct synaptic transmission (~ 5ms) (see chapter 1.3.1 & 4.1.2), but a transmission could be achieved by for example dendro-dendritic electric excitation/shunting, as can be found in the fly lobula **(Henning et al. 2008)**,

4.2| Ciliary Ca^{2+} Currents In the Johnston's Organ

4.2.1 | *iav1* Mutants Show Auditory Ca^{2+} Responses

The expression of a ciliary dilation marker advanced the recently developed technique of transcuticular Ca^{2+} imaging of chordotonal organs **(Kamikouchi & Wiek et al., 2010)**. The marker, DCX-EMAP:dsRed2, was used as an optical landmark, by which certain regions of the JO scolopidia were identified and distinguished. This allowed to image mechanically evoked Ca^{2+} responses in subregions of the distal cilium (see FIG 3.7 & 4.1). As the main protagonists of auditory transduction are known to locate to the cilium, I characterized the Ca^{2+} response properties of *iav1* mutant flies. Flies with *wt* antennal response characteristics show that the Ca^{2+} level rises from the tip of the cilium towards the NCB. Data approximation by a single and a double exponential rise to max indicates that a secondary process effects the Ca^{2+} response at the region of IAV localisation. Ca^{2+} responses in *iav1* mutant flies suggests, that mechanotransduction does not depend on IAV. Ca^{2+} responses in *iav1* mutant flies were 4 to 11 times smaller then in wildtype flies and the Ca^{2+} level is constant for all regions, seems consistent with the idea that IAV plays a role in signal amplification downstream of transduction **(Göpfert et al., 2006)**.

4.2.2 | Ca^{2+} Responses in *iav1* Mutants underline the Model of TRP-channel function by Göpfert et al.

These evidences underline the model for TRP-channel function in the *Drosophila* ear proposed by Göpfert et al **(2006)**. (see FIG 4.1). The modification of this model, suggested by Lehnert et al., posits that NAN/IAV are part of the transduction complex and that NOMPC is responsible for signal amplification **(Lehnert et al., 2013)**. Lehnert et al also rule out direct protein-protein interaction between NOMPC and NAN/IAV, as they are spatially divided by the ciliary dilation. Mechanotransduction is thought to work via ion channels that are directly gated mechanically.

Kim et al propose that NAN/IAV are gated by stretch and bending of the ciliary axoneme, as ciliary bending has been reported for the grasshopper FCO **(Liedtke et al ., 2005; Kim et al., 2007; Moran et al., 1977)**. NAN and IAV have been reported to be activated mechanically in vitro **(Kim et al., 2003, Gong et al., 2004)**, but further evidence is needed to confirm these results **(Lehnert et al., 2013)**. The evidences presented here and the previously reported loss of Ca^{2+} response in *nompC* mutants **(Effertz, Wiek & Göpfert, 2011)** support the assumption that NOMPC is a more promising candidate for the primary transduction channel than NAN/IAV.

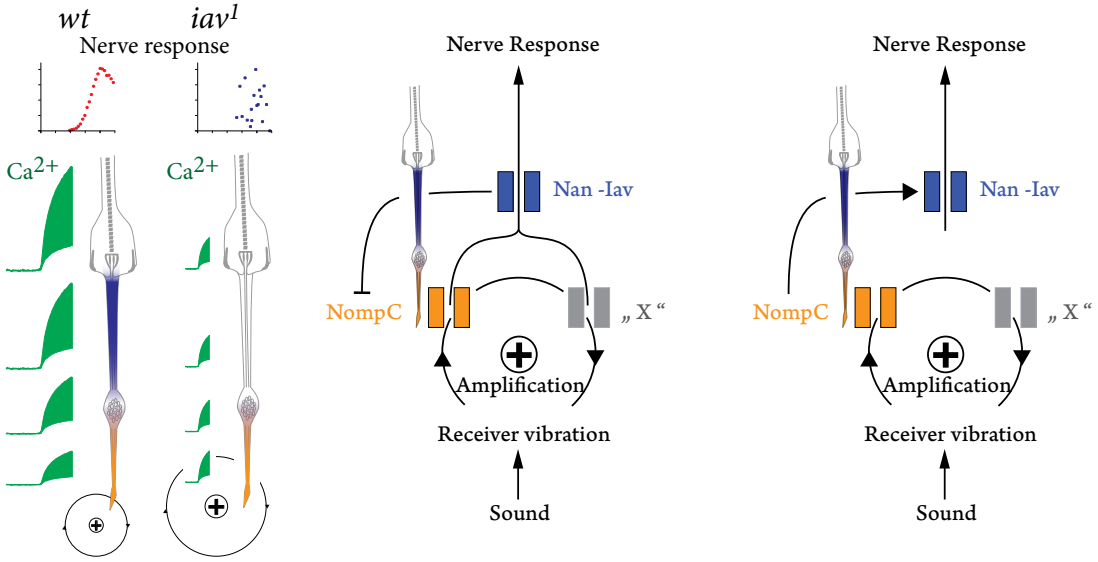

FIG 4.1 | Models of TRP-channel function in the *Drosophila* ear.

Left: Scheme of *wildtype* and *iav* mutant auditory response characteristics: iav^1 mutant flies show increased active amplification. Stimulation at the best frequency does not elicit any nerve potential, but evokes Ca^{2+} currents in the cilium and the NCB.

Göpfert Model: NOMPC might be an auditory transduction channel, as loss of these channels abolishes active amplification. Additional transduction channels "X" must exist, as reduced but not totally abolished sound evoked antennal nerve potentials are recorded in flies lacking NOMPC. The NAN/IAV heteromultimeric channel acts downstream of NOMPC and negatively controls amplification in a NOMPC dependent way. Loss of this control leads to excess amplification, resulting in self - sustained oscillations of the receiver. As judged from the complete loss of nerve potentials in *nan* and *iav* mutants, NAN/IAV is additionally required for propagating electrical signals from the transduction site to the antennal nerve.

Modified Model: Lehnert et al imply by the latency and speed of generator currents, recorded in giant fibre neurons, that the transduction complex is directly gated by mechanical force rather then a 2nd messenger cascade. They also propose that NAN/IAV is needed for sound evoked antennal field potential response and is therefore part of the transduction machinery and that NOMPC is modulating transduction.
Recordings of Ca^{2+} responses towards stimulation at the best frequency in iav^1 mutant flies contradict this proposition and underlines the model for auditory transduction suggested by Lu et al.
(see chapter 1.4.2 and 3.4 and FIG 1.5 & 1.6). [modified from Göpfert et al (2006) & Lu et al (2009)]

4.3 | Closing Remarks & Peroration

The method of *in vivo* transcuticular Ca^{2+} imaging I established and improved during the time of this thesis facilitates the dissection of functional properties of *Drosophila* neurons **(Kamikouchi & Wiek et al., 2010)**. Compared to electrode based nerve recordings this technique is less invasive and can be performed on intact animals. The unscathed nature of the specimen is especially important for the analysis of mechanosensory neurons, as their proper function depends on their suspension and the surrounding tissue.

I was able to show that neuronal responses of different organs can be monitored by this technique. During the time of this thesis I adjusted this technique to analyse specific properties of JO subsets and the effect of mutations on JO neurons **(Effertz, Wiek & Göpfert, 2011)**. By use of marker proteins expressed parallel to the Ca^{2+} sensor I could show that not only subsets of a sensory organ can be functionally dissected but also intrinsic functions of neurons can be monitored.

First evidence for FCO function was collected by *in vivo* transcuticular Ca^{2+} imaging and lead to behavioural experiments concerning the FCO function.

The behavioural experiments I designed suggest that Drosophila is sensitive to substrate vibrations and that the FCO is responsible for this sensitivity.

Higher spatial and time resolution provided for Ca^{2+} imaging are currently established by two photon microscopy and improved Ca^{2+} sensors. This would allow to identify the region of primary transduction in CHO's and to identify the functional properties of single scolopida in specific CHO.

Next to analysing mechanosensory cells in *Drosophila* I designed a recording Setup for a collaborative work with April Marrone, to analyse hyperthermic seizures and aberrant cellular homeostasis in *Drosophila* dystrophic muscles **(Marrone, Kucherenko, Wiek, Göpfert & Shcherbata, 2011)**.

5 | Abbreviations

AIC |	Akaikes information criterion
Cam |	Ca^{2+} binding domain of calmodulin
Cam 2.1 |	Cameleon 2.1
CNS |	central nervous system
CPG |	central pattern generator
CHO |	chordotonal organ
eCFP |	enhanced Cyan Fluorescent Protein
eYFP |	enhanced Yellow Fluorescent Protein
ES |	external sensory organ
EMAP |	Echinoderm Microtubule Associated Proteins
FFT |	Fast Fourier Transform
FCO |	femoral chordotonal organs
FRET |	Förster Resonance Energy Transfer
GECI |	genetically encoded Ca2+ indicators
GEVI |	genetically-encoded voltage indicator
GFP |	Green Fluorescent Protein
IAV / *iav* |	Inactive
iav^{1} |	*iav*^{1}*/ iav1;Cam2.1,Cam2.1;NP0761/DCX-EMAP:dsRed2*
iav1/FM7c |	*iav*^{1}*/FM7c;Cam2.1,Cam2.1;NP0761/DCX-EMAP:dsRed2*
Ca2+ |	intracellular ionic calcium
JO |	Johnston´s Organ
LDV |	Laser Doppler Vibrometer
Math1 |	mouse atonal homologue 1
MD |	multidenditic neurons
NAN / *nan* |	Nanchung
NCB |	Nerve Cell Body
NOMPC |	No mechano receptor potential C; also called TRPN1
ΔR/R0 |	Ratio change
ROI |	regions of interest
SOP |	sensory organ precursor cells
TRP |	transient receptor potential
TRPV |	transient receptor potential vanilloid
UAS |	upstream activating sequence
wt |	wild-type

|| *Genes* are written in *italic* and PROTEINS are written in CAPTION letters ||

6 | Literature

A

Adams et al (2000)

Review:The Genome Sequence of *Drosophila* melanogaster
Science, Vol. 287 no. 5461 : 2185-2195

Akaike H (1973)

Information theory and an extension of the maximum likelihood principle.
In: B. N. Petrov (Hrsg.) u.A.:
Proceedings of the Second International Symposium on
Information Theory Budapest: Akademiai Kiado 1973. S. 267-281

Albert JT, Nadrowski B, Göpfert MC (2007)

Mechanical signatures of transducer gating in the drosophila ear.
Curr Biol Vol 17:1000–1006.

Albert JT, Nadrowski B, Göpfert MC (2007)

Drosophila mechanotransduction–linking proteins and functions.
Fly (Austin) Vol 1:238–241.

Altner H and Thies G.(1984)

Internal proprioceptive organs of the distal antennal segments in Allacma fusca (L.)(Collembola : Sminthuridae): proprioceptors phylogenetically derived from sensillum bound exteroceptors.
Int. J. Insect Morphol. Embryol., Vol 13: 315-30

Amarasinghe AK, MacDiarmid R, Adams MD, Rio DC (2001)
An invitro-selected rna-binding site for the kh domain protein psi acts as a splicing inhibitor element.
RNA Vol 7:1239–1253.

B

Bang AG & Posakony JW(1992)
The*Drosophila* gene Hairless encodes a novel basic protein that controls alter native cell fates in adult sensory organ development.
Genes Si Dev. vol 6: 1752-1769.

Bässler U (1993)
The femur – tibia control system of stick insects – a model system for the study of the neural basis of joint control.
Brain Res Rev 18, 207-226

Bässler U (1986)
Afferent control of walking movements in the stick insect Cuniculina impigra.
II. Reflex reversal and the release of the swing phase in the restrained foreleg.
J.Comp.Physiol.A Vol 158: 351–362.

Bässler U (1988)
Functional principles of pattern generation for walking movements of stick insect forelegs: the role of the femoral chordotonalorgan afferences.
J. Exp. Biol. Vol 136: 125–147.

Bechstedt S, Albert JT, Kreil DP , Müller-Reichert T, Göpfert MC & Howard J(2010)
A doublecortin containing microtubule-associated protein is implicated in mechanotransduction in*Drosophila* sensory cilia.
Nature Communications 1,Article number:11

Bell PD (1980)
TRANSMISSION OF VIBRATIONS ALONG PLANT STEMS: IMPLICATIONS FOR INSECT COMMUNICATION
NewYORK ENTOMOLOGICAL SOCIETY, VOLLXXXVIII(3):210-216

Berridge MJ (1998)
Neuronal Calcium Signaling
Neuron, Vol 21: 13-26,

Boekhoff-Falk G (2005)
Hearing in*Drosophila*: development of johnston's organ and emerging parallels to vertebrate ear development.
Dev Dyn Vol 232:550–558.

Brand AH & Perrimon N (1993)
Targeted gene expression as a means of altering cell fates and generating dominant phenotypes.
Development Vol 118:401–415.

Branson K, Robie A A, Bender J, Perona P, Dickinson M (2009)
High – throughput ethomics in large groups of*Drosophila*.
Nature Methods Vol 6: 451-457

Büschges (1994)
The physiology of sensory cells in the ventralscoloparium of the stick insect femoral chordotonal organ.
J. exp. Biol. Vol 189:285–292

Büschges A (2005)
Sensory control and organization of neural networks mediating coordination of multisegmental organs for locomotion.
Journal of neurophysiology Vol 93(3):1127-35

C

Castle WE, Carpenter FW, Clark AH, Mast SO & Barrows WM (1906)
The effects of inbreeding, cross-breeding, and selection upon the fertility and variability of Drosophila.
Proc. Am. Acad. Arts Sci., Vol 41:729-86.

Caldwell JC & Eberl DF (2002)
Towards a molecular understanding of *Drosophila* hearing.
Journal of Neurobiology 53: 172-189.

Chalfie M , Tu Y, Euskirchen G, Ward WW, and Prasher DC (1994)
Green fluorescent protein as a marker for gene expression
Science, Vol 263, Issue 5148: 802-805.

Cheng Li E. , Wei Song, Loren L. Looger, Lily Yeh Jan, Yuh Nung Jan, (2010)
The Role of the TRP Channel NompC in *Drosophila* Larval and Adult Locomotion,
Neuron, Vol 67(3): 373-380

D

DiCaprio, Wolf and Büschges A (2002)
Activity-Dependent Sensitivity of Proprioceptive Sensory Neurons in the Stick Insect Femoral Chordotonal Organ
J Neurophysiol , Vol 88: 2387–2398

E

Eberl DF & Boekhoff-Falk G (2007)
Development of Johnston's organ in *Drosophila*.
Int. J. Dev. Biol., Vol 51: 679-687.

Effertz T, Wiek R, Göpfert MC (2011)
Nompc trp channel is essential for *Drosophila* sound receptor function.
Curr Biol Vol 21:592–597.

Ewing A, Bennet-Clark H (1968)
The courtship songs of drosophila.
Behaviour Vol 31:288–301.

Ewing AW, Miyan JA (1986)
Sexual selection, sexual isolation and the evolution of song in the *Drosophila repleta* group of species.
Animal Behaviour Vol 34:421 – 429.

F

Fabre CG, Hedwig B, Conduit G, Lawrence PA, Goodwin Sf, Casal J (2012)
Substrate-Borne Vibratory Communication during Courtship in *Drosophila melanogaster*
Curr Biol Vol 22 (22): 2180–2185

Feinberg EH, Vanhoven MK, Bendesky A, Wang G, Fetter RD,
Shen K, Bargmann CI (2008)
GFP Reconstitution Across Synaptic Partners (GRASP) defines cell contacts and synapses in living nervous systems.
Neuron. Vol 57(3): 353-63

Fiala A & Spall T (2003)
In vivo calcium imaging of brain activity in*Drosophila* by transgenic cameleon expression.
Sci. STKE Vol 174, PL6

Fiala A, et al. (2002)
Genetically expressed cameleon in *Drosophila* melanogaster is used to visualize olfactory information in projection neurons.
Curr Biol Vol 12:1877–1884.

Field LH, Matheson T.(1998)
Chordotonal organs of insects
Advances in Insect Physiology Vol 27:1-230

G

Gong Z et al (2004)
Two Interdependent TRPV Channel Subunits, Inactive and Nanchung, Mediate Hearing in Drosophila
The Journal of Neuroscience, Vol 24(41):9059 –9066

Göpfert MC, and RobertD (2001)
Biomechanics. turning the key on *Drosophila* audition.
Nature, Vol 411:908.

Göpfert MC, and RobertD (2002)
The mechanical basis of*Drosophila* audition.
The Journal of Experimental Biology Vol 205: 1199–1208.

Göpfert MC, and RobertD (2002)
Motion generation by Drosophila mechanosensory neurons.
PNAS, Vol 100 (9): 5514–5519.

Göpfert MC, Humphris ADL, Albert JT , Robert D and Hendrich O (2005)
Power gain exhibited by motile mechanosensory neurons in*Drosophila* ears
PNAS, Vol 102 (2) : 325-330

Göpfert MC, Albert JT, Nadrowski B, & Kamikouchi A (2006).
Specification of auditory sensitivity by *Drosophila* TRP channels.
Nat Neurosci, Vol 9(8): 999–1000.

GraberV (1882)
Die chordotonalen Sinnesorgane und das Gehör der Insekten
Arch. mikr. Anat., Vol 20: 506–640

Greenspan RJ (2004)
Fly pushing 2nd Edition
Cold Spring Harbor Laboratory Press

Grienberger C, Konnerth A (2012)
Imaging Calcium in Neurons
Neuron Vol 73: 862 - 885

Grünert U & Gnatzy W(1987)
K^+ and Ca^{2+} in the receptor lymph of arthropod cuticular mechanoreceptors.
J. Comp. Physiol., Vol 161:329–333.

H

Hall JC (1994)
The mating of a fly.
Science Vol 264(5166): 1702–1714.

Harris WA, Stark WS, Walker JA (1976)
Genetic dissection of the photoreceptor system in the compound eye of *Drosophila melanogaster*.
J Physiol (london) Vol 256: 415-439

Heisenberg M & Wolf R (1984)
Vision in *Drosophila* (Genetics of Microbehavior)
Springer -Verlag (Berlin, Heidelberg, NewYork, Tokio):ISBN 3-540-136851

Hennig M, Möller R, Egelhaaf M (2008)
Distributed Dendritic Processing Facilitates Object Detection:
A Computational Analysis on the Visual System of the Fly
PLoS ONE Vol 3(8): e3092.

Hill PSM (2001)
Vibration and Animal Communication: A Review.
Amer,Zool., Vol 41:1135-1142

Hofmann T und Koch UT (1985)
Acceleration receptors in the femoral chordotonal organ of the stick insect,
Cuniculina impigra.
J. exp. Biol. Vol 114:225–237

Hofmann T, Koch UT und Bässler U (1985)
Physiology of the femoral chordotonal organ in the stick insect,
Cuniculina impigra.
J. exp. Biol. Vol 114, 207–223.

Howard J, Bechstedt S (2004)
Hypothesis: a helix of ankyrin repeats of the nompc-trp ion channel is the
gating spring of mechanoreceptors.
Curr Biol Vol 14: R224–R226.

Hoy RR, Hoikkala A, Kaneshiro K (1988)
Hawaiian courtship songs:
evolutionary innovation in communication signals of drosophila.
Science Vol 240:217–219.

I

Ito K, Suzuki K, Estes P, Ramaswami M, Yamamoto D, Strausfeld NJ (1998)
The organization of extrinsic neurons and their implications in the
functional roles of the mushroom bodies in Drosophila melanogaster Meigen.
Learn. Mem., Vol 5:52–77.

J

Jan YH & Jan LY (1994)
Genetic control of Cell fate specification in*Drosophila* peripheral
Nervous System.
Annu.Rev.Genet., Vol 28:373-93.

Jarman AP, Yan S, Jan LY and Jan YN (1995)
Role of the proneural gene, atonal, in formation of*Drosophila* chordotonal organs and photoreceptors.
Development, Vol 121:2019-2030.

Johnston (1855)
Auditory apparatus of the culex mosquitoes.
Q.J.Microsc 3:97–102.

K

Kamikouchi A(2006)
Comprehensive Classification of the Auditory Sensory Projections in the Brain of the Fruit Fly *Drosophila* melanogaster.
The Journal of comparative Neurology, Vol 499:317–356.

Kamikouchi A et al (2009)
The neural basis of*Drosophila* gravity-sensing and hearing.
Nature Vol 458(7235):165-71.

Kamikouchi A, Wiek RJ, et al (2010)
Transcuticular optical imaging of stimulus-evoked neural activities in the *Drosophila* peripheral nervous system.
Nature Protocols Vol 5: 1229 - 1235

Keil TA (1997)
Functional morphology of insect mechanoreceptors.
Microsc. Res. Tech., Vol 39:506-31.

Kernan M., Cowan D., Zuker C. (1994)
Genetic dissection of mechanosensory transduction: mechanoreception-defective mutations of Drosophila.

Neuron Vol 12:1195–1206.

Kernan MJ (2007)
Mechanotransduction and auditory transduction in*Drosophila*.
Pflugers Arch - Eur. J. Physiol. Vol 454: 703-720.

Kidwell MG, Kidwell JF, Sved JA (1977)
Hybrid dysgenesis in *Drosophila* melanogaster: A syndrome of aberrant traits including mutation, sterility and male recombination.
Genetics Vol 86: 813–833.

Kim C (2007)
Chapter 17:
TRPV Family Ion Channels and Other Molecular Components
Required for Hearing and Proprioception in Drosophila
TRP Ion Channel Function in Sensory Transduction and
Cellular Signaling Cascades.
Liedtke WB, Heller S, editors.
Boca Raton (FL): CRC Press; 2007.

Klagges B. R. E., Heimbeck G., Godenschwege T.A., Hofbauer A., Pflugfelder G.O., Reifegerste R., Reisch D., Schaupp M., Buchner S., Buchner E.(1996)
Invertebrate Synapsins: A Single Gene Codes for Several Isoforms in Drosophila.
The Journal of Neuroscience, Vol 16:3154-3165.

Kralj JM, Douglass AD, Hochbaum DR, Maclaurin D & Cohen AE (2012)
Optical recording of action potentials in mammalian neurons using a microbial rhodopsin
Nature Methods Vol 9: 90–95

L

Lee G, et al. (2006)
Nanospring behaviour of ankyrin repeats.
Nature Vol 440:246–249.

Lee J, Moon S, Cha Y, Chung YD (2010)
Drosophila trpn(=nompc) channel localizes to the distal end of mechanosensory cilia.
PLoS One 5: e11012.

Lehnert BP, Baker AE, Gaudry Q, Chiang AS, Wilson RI (2013)
Distinct roles of TRP channels in auditory transduction and amplification in Drosophila.
Neuron. Vol 77(1): 115-28

Liang X, Madrid J, Saleh HS, Howard J (2011)
Nompc, a member of the trp channel family, localizes to the tubular body and distal cilium of *drosophila* campaniform and chordotonal receptor cells.
Cytoskeleton (Hoboken) Vol 68: 1–7.

Liedtke W, Kim C (2005)
Functionality of the TRPV subfamily of TRP ion channels: add mechano-TRP and osmo-TRP to the lexicon!
Cell Mol Life Sci. Vol 62(24): 2985-3001.

Lu Q, Senthilan PR, Effertz T, Nadrowski B, Göpfert MC (2009)
Using Drosophila for studying fundamental processes in hearing
Integr. Comp. Biol. Vol 49 (6): 674-680.

M

McIver SB (1985)
Mechanoreception.
Comprehensive Insect Physiology, Biochem. and Pharmacology. Vol 6:71-132

Meigen JW (1830).
Systematische Beschreibung der bekannten europäischen zweiflügeligen Insekten.
Sechster Theil mit zwölf Kupfertafeln. - pp. I-XI [= 1-11], 1-401, [3].
Hamm. (Schulz).

Metaxakis A, Oehler S, Klinakis A & Savakis C (2005)
Minos as a genetic and genomic tool in *Drosophila* melanogaster.
Genetics, Vol 171(2): 571-81

Miyawaki A, Llopis J, Heim R, McCaffery JM, Adams JA, Ikura M, and Tsien RY (1997)
Fluorescent indicators for Ca^{2+} based on green fluorescent proteins and calmodulin.
Nature, Vol 388: 882–887

Miyawaki A, Griesbeck O, Heim R, and Tsien, RY (1999)
Dynamic and quantitative Ca^{2+} measurements using improved cameleons.
Proc. Natl. Acad. Sci. USA, Vol 96: 2135–2140.

Montell C, et al. (2002)
A unified nomenclature for the superfamily of trp cation channels.
Mol Cell Vol 9: 229–231.

Montell C (2005)
The TRP Superfamily of Cation Channels

Sci. STKE (272), re3. [DOI: 10.1126/stke.2722005re3]

Morgan TH (1913)
Heredity & Sex, The Jesup Lectures
Columbia University Press

Moran DT, Varela FJ and Rowley JC 3rd (1997)
Evidence for active role of cilia in sensory transduction.
Proc Natl Acad Sci USA. Vol 74(2): 793–797.

N

Nadrowski B, Göpfert MC (2009)
Modeling auditory transducer dynamics.
Curr Opin Otolaryngol Head Neck Surg Vol 17:400–406.

Narda RD (1966)
Analysis of the stimuli involved in courtship and mating in d. malerkotliana (sophophora, *Drosophila*).
Animal Behaviour, Vol 14: 378 –383.

Nishino H, Field LH (2003)
Somatotopic mapping of chordotonal organ neurons in a primitive ensiferan, the New Zealand tree weta Hemideina femorata: II. complex tibial organ
The Journal of Comparative Neurology, Vol 464 (3): 327–342

O

Orlovsky GN, Deliagina TG, Grillner S (1999)
Neuronal control of locomotion.
Oxford: Oxford UP.

P

Pearson KG (1995)
Proprioceptive regulation of locomotion.
Curr. Opin. Neurobiol Vol 5: 786–791

Polytec Homepage
Basic Principles of Vibrometry
http://www.polytec.com/int/solutions/vibration-measurement/
basic-principles-of-vibrometry/

R

Robie AA, Straw AD, Dickinson MH (2010)
Object preference by walking fruit flies, *Drosophila melanogaster*, is mediated by vision and graviperception.
J Exp Biol. ,Vol 213(Pt 14):2494-506.

Ryder E & Russell S (2003)
Transposable elements as tools for
genomics and genetics in *Drosophila*.
Brief Funct Genomic Proteomic, Vol 2:57–71.

Riemensperger T, Pech U, Dipt S & Fiala A (2012)
Optical calcium imaging in the nervous system of *Drosophila melanogaster*
Biochimica et Biophysica Acta (BBA) Vol 1820:1169–1178

S

Schilcher F (1976)
The behavior of cacophony, a courtship song mutant in *Drosophila melanogaster*.
Behav Biol, 17(2), 187–196.

Senthilan PR, Piepenbrock D, Ovezmyradov G, Nadrowski B, Bechstedt S, Pauls S, Winkler M, Möbius W, Howard J, Göpfert MC (2012)
Drosophila Auditory Organ Genes and Genetic Hearing Defects
Cell Vol 150 (5): 1042 - 1054)

Shanbhag SR, Singh K & Singh N (1992)
Ultrastructure of the FEMORAL CHORDOTONAL ORGANS and their novel synaptic Organization in the Legs of*Drosophila* melanogaster Meigen (Diptera : Drosophilidae).
Int. J. Insect Morphol. & Embryol., Vol 21: 311-322.

Shorey HH (1962)
Nature of the sound produced by*Drosophila* melanogaster during courtship.
Science, Vol 137:677–678.

Snodgrass RD(1926)
The morphology of insect sense organs and the sensory nervous system.
Smithson. Misc. Collect., Vol 77: 1-80.

Sotomayor M, Corey DP, Schulten K (2005)
In search of the hair-cell gating spring elastic properties
of ankyrin and cadherin repeats.
Structure Vol 13: 669–682.

Spieth H (1952)
Mating behavior within the genus *Drosophila*.
Bulletin of the American Museum of Natural History, Vol 99: 401–474.

T

Thibault ST et al (2004)
A complementary transposon tool kit for *Drosophila* melanogaster
using P and piggyBac
Nature Genetics, Vol 36: 283 - 287 (2004)

Todi SV, Sharma Y, Eberl DF (2004)
Anatomical and molecular design of the *Drosophila* antenna as a flagellar
auditory organ.
Microsc Res Tech Vol 63:388–399.

Tracey WD Jr, Wilson RI, Laurent G, Benzer S.(2003)
Painless, a*Drosophila* gene essential for nociception.
Cell, Vol 113(2):261-73.

W

Chu-Wang IW and Axtell RC (1972)
Fine structure of the terminal organ of the house fly larva,
Musca domestica (L). Z. Zellforsch., Vol 127: 287-305.

Wang VY, Hassan BA, Bellen HJ, Zoghbi HY (2002)
Drosophila atonal fully rescues the phenotype of Math1 null mice:
new functions evolve in new cellular contexts.
Curr Biol., Vol 12(18):1611-6.

Wiek RJ (2008) (Matrikel. Nr.: 3606899)
Funktion und Morphologie chordotonaler Sensillen im Bein der Taufliege
Drosophila melanogaster
Als Diplomarbeit vorgelegt dem Vorsitzenden des Prüfungsausschusses für die
Diplomprüfung im Fach Biologie.
Angefertigt bei Prof. Dr. rer. nat. Martin C. Göpfert
Universität zu Köln.

Y

Yack JE (2004)
The structure and Function of Auditory Chordotonal Organs in Insects.
Microscopy Research and Technique, Vol 63:315-337.

Yannoni YM and White K (1999)
Domain necessary for*Drosophila* ELAV nuclear localization:
function requi res nuclear ELAV.
Journal of Cell Science, Vol 112:4501-4512.

Young D (1973)

Fine structure of the sensory cilium of an insect auditory receptor.
J. Neurocytol., Vol 2:47-58. Chu-Wang and Ax-tell, 1972;

Yoshihara M, Ito K

Improved Gal4 screening kit for large-scale generation of enhancer-trap strains.
Drosoph. Inf. Serv. 2000, Vol 83:199–202.

Z

Zacharuk RY and Albert PJ (1978)

Ultrastructure and function of scolopophorous sensilla in the mandible of an elasterid larva (Coleoptera).
Can. J. Zool., Vol 56:246-59.

Zill S, Schmitz J, Büschges A (2004)

Load sensing and control of posture and locomotion.
Arth. Struct. Dev., Vol 33: 273–286.

7 | Acknowledgements

First of all I have to thank Martin Göpfert who allowed me to leave the beaten path and work independently. He encouraged me to design my own experiments and helped me with a different point of view when I got stuck in a one way road. Next to scientific issues he always had an ear for personal concerns.
I have to thank Thomas Effertz, with whom I worked on several projects and who was always critic so that I had to improve myself.
I have to thank Björn Nadrowski, who helped me to think out of the box and to address problems with a mathematical approach.
I have to thank Simon Lu who introduced me to data analysis and was always fun to talk to.
I want to thank David Piepenbrock for friendship and competition, in science and sports (and partying).
I have to thank Bart Geurten, whom I could always ask for help and cologne-gossip.
I have to thank all who provided the Laboratories backbone, like Gudrun Mathes, Steffi Pauls, Heribert Gras, Ralf Heinrich, Christian Spalthoff and Andreas Stumpner.
I also thank all my desk neighbours: Pingkalai Senthilan, Georg Raiser, Philip Jähde, Krissy Corthals and all the Bachelor and Master students.

I especially have to thank the new friends I found in Göttingen, as there are Simone Michalek, Sebastian Wagner, Tinki Severs, Alexander Dirk, Mona, Robin and all the others I can not mention here.
A special thank goes to Lena who always supported me and with whom I went through thick and thin. I also have to thank Lenas parents Marion and Wolfgang who accommodated me and Lena when we jumped out of the frying pan into the fire.

At least I have to thank my parents Henny Schwartkopff- Wiek and Eberhard Wiek, my Grandmother Jutta Peters and my sister Nora who always supported and comforted me. I also have to thank my lately departed uncle Prof.Dr. Bodo Schwartzkopff, who was the first scientist I knew.

8 | Personal Information

8.1 | Curriculum Vitae

Name:	Robert Jago Wiek
Date of birth:	20.04.1982
Place of Birth:	Münster, NRW, Germany

Education

2009- present:	PhD Student, Georg-August University Göttingen Department for Cellular Neurobiology
Supervisor:	Prof. Dr. Martin C. Göpfert
Thesis title:	A Functional Characterization of *Drosophila* Chordotonal Organs
2007-2008:	Diploma Thesis, University of Cologne Institut for Zoology
Supervisor:	Prof. Dr. Martin C. Göpfert
Diploma title:	Funktion und Morphologie chordotonaler Sensillen im Bein der Fruchtfliege *Drosophila melanogaster*
2002-2008	Diploma Studies in Biology, University of Cologne
2001-2002	Diploma Studies in Chemistry, University of Cologne
2001	Allgemeine Hochschulreife (A level), Gymnasium Rodenkirchen, Cologne

8.2 | Conferences & Symposia

2012 - 2013	Organisation Committee Neuro Dowo 2013, University Göttingen
13. - 16. 03 2013	NWG, Göttingen 2013 (Poster)
01.-04.08.2012	Neuro Dowo, University Marburg (Presentation)
23. - 27. 03 2011	NWG, Göttingen 2011 (Poster)
26.- 27.08.2010	Regional Drosophila Meeting, Göttingen (Poster)
March 2010	Neurobiological Practical Course - HEARING (University Tübingen)
04.-05.02.2010	Crossroads in Biology, Univerität zu Köln (Poster)
2009-2010	Organisation Committee `Neuroprosthetics: From Sensorimotor Research to Applications´, GGNB, Göttingen

8.3 | Publications

Effertz T, Wiek R, Göpfert MC (2011)
Nompc trp channel is essential for *Drosophila* sound receptor function.
Curr Biol Vol 21:592–597.

AK Marrone, MM Kucherenko, R Wiek, MC Göpfert, HR Shcherbata (2011)
Hyperthermic seizures and aberrant cellular homeostasis in *Drosophila* dystrophic muscles
Scientific reports 1

Kamikouchi A, Wiek RJ, et al (2010)
Transcuticular optical imaging of stimulus-evoked neural activities in the *Drosophila* peripheral nervous system.
Nature Protocols Vol 5: 1229 - 1235

*

*

*

*

*